Merging on the Fly Without Retraining: A Sequential Approach to Scalable Continual Model Merging

Anke Tang[1] **Enneng Yang**[2] **Li Shen**[2*] **Yong Luo**[1*] **Han Hu**[3] **Lefei Zhang**[1]
Bo Du[1] **Dacheng Tao**[4]
[1]School of Computer Science, National Engineering Research Center of Multimedia Software and Hubei Key Laboratory of Multimedia and Network Communication Engineering, Wuhan University, Wuhan, China
[2]Shenzhen Campus of Sun Yat-sen University, China [3]Beijing Institute of Technology, Beijing, China
[4]Nanyang Technological University, Singapore
{anketang, luoyong, zhangleifei, dubo}@whu.edu.cn yangenn@mail.sysu.edu.cn
hhu@bit.edu.cn {mathshenli, dacheng.tao}@gmail.com

Abstract

Deep model merging represents an emerging research direction that combines multiple fine-tuned models to harness their specialized capabilities across different tasks and domains. Current model merging techniques focus on merging all available models simultaneously, with weight interpolation-based methods being the predominant approach. However, these conventional approaches are not well-suited for scenarios where models become available sequentially, and they often suffer from high memory requirements and potential interference between tasks. In this study, we propose a training-free projection-based continual merging method that processes models sequentially through orthogonal projections of weight matrices and adaptive scaling mechanisms. Our method operates by projecting new parameter updates onto subspaces orthogonal to existing merged parameter updates while using an adaptive scaling mechanism to maintain stable parameter distances, enabling efficient sequential integration of task-specific knowledge. Our approach maintains constant memory complexity to the number of models, minimizes interference between tasks through orthogonal projections, and retains the performance of previously merged models through adaptive task vector scaling. Extensive experiments on CLIP-ViT models demonstrate that our method achieves a 5-8% average accuracy improvement while maintaining robust performance in different task orderings. Code is publicly available at https://github.com/tanganke/opcm/.

1 Introduction

With the continued expansion of the scale of foundation models, the demand for efficient model development becomes increasingly pressing [104, 94]. Model merging, as a promising approach to address this challenge, aims to combine multiple fine-tuned models to harness their specialized capabilities in different tasks and domains [43, 92, 50, 35]. Recent studies have demonstrated the effectiveness of model merging in various scenarios, from combining language models with different task expertise [91, 98, 51] to merging vision models trained in distinct domains [86, 73].

The predominant approach to model merging is weight interpolation, which combines model parameters through weighted averaging of the individual models' weights [29, 82]. This method can be formalized as $\theta_{\text{merged}} = \theta^{(0)} + \sum_{i=1}^{n} \alpha_i(\theta^{(i)} - \theta^{(0)})$, where $\theta^{(0)}$ and $\theta^{(i)}$ represent the parameters

*Corresponding authors.

39th Conference on Neural Information Processing Systems (NeurIPS 2025).

of the pre-trained model and the i-th expert model, respectively, and α_i are the interpolation coefficients, which can be applied task- or layer-wise [52, 96]. Theoretically, the effectiveness of weight interpolation-based merging methods is mainly influenced by two factors: data heterogeneity (the diversity of training set distribution between expert models) and training heterogeneity (differences in hyperparameter settings and optimization dynamics) [59, 78].

However, existing model merging approaches face several fundamental limitations that hinder their practical application and can be revisited from a continual merging perspective. Firstly, current methods typically require concurrent access to all models during the merging process, resulting in significant memory overhead that scales linearly with the number of models being merged [69]. Secondly, the law of commutation in model merging may not hold in continual merging scenarios, where the order of merging models is crucial and can affect the performance of the final merged model. This results in additional challenges for the algorithm design. Third, sequential model availability is a common real-world scenario and lacks attention in existing studies. Last, many current approaches necessitate additional training phases or extensive hyperparameter optimization, introducing substantial computational costs or validation demands [33, 74, 107, 42].

To address these challenges, we propose the Orthogonal Projection-based Continual Merging (OPCM) method which enables a sequential merging as new models become available. Our approach consists of three key features: (1) By maintaining only the current merged and pre-trained models, we sequentially process new models, achieving constant memory complexity $O(|\theta|)$. (2) A projection-based merging mechanism processes parameter updates through orthogonal projections to minimize parameter interference between the incoming and merged models. (3) An adaptive time-varying scaling factor that dynamically adjusts the contribution of each model during the merging process to maintain stable performance, making the method robust to different merging orders. Together, these features enable OPCM to achieve training-free and memory-efficient merging.

Our approach is built upon two key insights: (1) the use of orthogonal projections effectively minimizes interference between different tasks while preserving the specialized capabilities of each model, and (2) an adaptive scaling strategy keeps an approximately constant distance between the merged model and the pre-trained model, ensuring stable performance of the merged model.

In summary, our contributions are (1) We provide a formal mathematical framework for sequential model merging, and discuss its relationship with existing model merging methods. (2) We propose a training-free projection-based continual merging method that processes models sequentially through orthogonal projections and adaptive scaling mechanisms. (3) We conduct extensive experiments on image classification tasks to demonstrate the effectiveness of our method and show 5-8% better accuracy on average while remaining consistently robust regardless of how tasks are ordered.

2 Related Work

Deep Model Fusion is scalable and effective in various scenarios, including language modeling [106, 79, 81], vision modeling [97, 27], and multimodal modeling [94, 8]. Following [75], deep model fusion techniques can be categorized into three types: model ensemble [68, 3, 48], model merging [43], and model mixing [92, 38]. In this study, we focus on model merging, which does not change the model architecture or introduce inference costs.

(1) *Weight interpolation-based model merging* is one of the most straightforward and intuitive methods for merging model parameters. This approach is largely based on the observation of mode connectivity, which suggests that different solutions within the parameter space can be connected by paths that maintain a consistently low loss [22, 17, 21, 101]. This method assumes that the models being merged lie in similar regions of the loss landscape, allowing for a seamless transition between them without significantly increasing the loss [30, 52, 86, 2, 29, 67]. In addition to its application in multi-task model fusion, weight interpolation can also be utilized during the preference alignment phase in LLM training [103, 46, 7, 25, 61], data-mixing [93, 1], auxiliary-task learning [31], and deep multi-objective optimization [64, 9, 76, 15]. (2) *Alignment-based model merging* represents another approach that focuses on merging models through the reduction of parameter or feature disparities. Current research includes activation and weight matching [72, 33, 95, 36, 90, 54], utilizing channel-wise graph matching [47], and applying permutation invariant [2, 44].

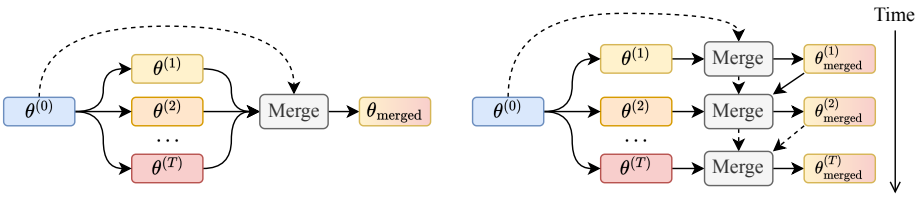

(a) Conventional model merging (b) Continual model merging

Figure 1: Comparison between conventional and continual model merging approaches. (a) Conventional model merging requires simultaneous access to all expert models, performing merging in a single step. (b) Continual model merging processes models sequentially as they become available.

However, the above methods require all models to be available simultaneously for merging, which limits their applicability. In contrast, our approach enables the continual merging of sequentially arriving models with higher memory efficiency.

Continual Learning addresses scenarios where models must sequentially learn new tasks while maintaining performance on previously acquired knowledge [84, 105]. This challenging paradigm has led to several key approaches: memory-based methods that store past samples [49, 6, 5], architecture-based methods that modify network structures [66, 20, 99], regularization-based methods involve the addition of regularization loss terms [37, 102], subspace-based methods that use lower-dimensional projections [19, 16], and Bayesian methods via incorporating uncertainty estimation [56]. However, the aforementioned methods are all based on learning from the original data. In contrast, the continual merging approach proposed in this paper allows us to directly merge a sequence of models (i.e., tasks) arriving in a stream, offering an orthogonal perspective to continual learning.

3 Rethinking Model Merging From a Continual Learning Perspective

In this section, we present a novel perspective on multi-task model merging through the lens of continual learning, wherein task-specific models are obtained sequentially rather than simultaneously.

3.1 Problem Setup

Formally, let $f_{\theta^{(0)}} : \mathcal{X} \to \mathcal{Y}$ denote the pre-trained model parameterized by $\theta^{(0)}$, where $\mathcal{X}$ represents the input space and $\mathcal{Y}$ represents the output space. Consider T task-specific models: $\{f_{\theta^{(1)}}, f_{\theta^{(2)}}, \ldots, f_{\theta^{(T)}}\}$, each fine-tuned from the pre-trained model $f_{\theta^{(0)}}$ using the corresponding data set D_i for task i. Each model may incorporate a task-specific head $h_{\phi_i} : \mathcal{Y} \to \mathcal{Z}_i$. Our objective is to construct a unified model $f_{\theta_{\text{merged}}} : \mathcal{X} \to \mathcal{Y}$ that maintains high performance in all T tasks while preserving task-specific heads $\{h_{\phi_i}\}_{i=1}^{T}$. Initially, we define the conventional versus continual model merging approaches in formal terms and subsequently explore the challenges and current solutions from a continual learning perspective. In Figure 1, we provide a visual comparison between conventional and continual model merging techniques, highlighting their distinctive approaches.

Definition 3.1 (Conventional Model Merging)**.** Conventional model merging approaches predominantly address scenarios where all expert models are available simultaneously, executing the merge operation in a single step. This process can be formally expressed as follows:

$$\theta_{\text{merged}} = \text{Merge}(\theta^{(0)}; \theta^{(1)}, \theta^{(2)}, \ldots, \theta^{(T)}). \tag{1}$$

Definition 3.2 (Continual Model Merging)**.** Task-specific models are introduced progressively over time in the continuous model merging scenario. Model merging occurs incrementally in this paradigm as each new task-specific model becomes available. Specifically, at step t, we merge the current merged model parameterized by $\theta^{(t-1)}_{\text{merged}}$ with the newly trained task-specific model parameterized by $\theta^{(t)}$, yielding an updated merged model parameterized by $\theta^{(t)}_{\text{merged}}$. This process can be formalized as:

$$\theta^{(t)}_{\text{merged}} = \text{ContinualMerge}(\theta^{(t-1)}_{\text{merged}}; \theta^{(0)}, \theta^{(t)}), \ t \geq 2, \tag{2}$$

where typically $\theta^{(1)}_{\text{merged}} = \theta^{(1)}$ is initialized as the first expert model and $\theta^{(t)}_{\text{merged}}$ aims to minimize the expected risk $\theta^{(t)}_{\text{merged}} = \arg\min_\theta \mathbb{E}_{(x,y)\sim\mathcal{D}_1\cup\ldots\mathcal{D}_t} \mathcal{L}_t\left(f_\theta(x), y\right)$.

3.2 Opportunities & Challenges in Continual Merging

Storage and memory efficiency is a significant advantage of continual merging over traditional merging methods. In continual merging, at each step t, only a fixed number of models need to be stored: the current merged model, the new model to be merged, and optionally the pre-trained base model. This approach leads to a constant memory complexity of $O(|\theta|)$, where $|\theta|$ represents the size of an individual model. Crucially, this memory requirement remains constant, regardless of the total number of downstream tasks T involved. In contrast, as shown in Figure 2, conventional merging methods typically involve maintaining all models, which results in a linear memory complexity of $O(T|\theta|)$.

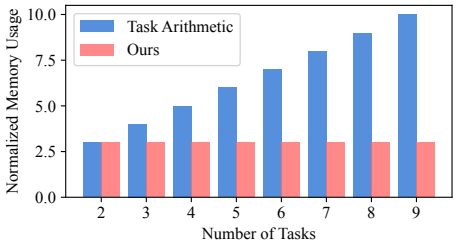

Figure 2: Memory complexity of task arithmetic [29] and our method.

The law of commutation in model merging refers to the property that the sequence in which models are combined does not influence the outcome of the merged model. Formally, this commutative property is described by the equation for standard merging techniques as the following holds:

$$\text{Merge}(\theta^{(0)}; \theta^{(i)}, \theta^{(j)}) = \text{Merge}(\theta^{(0)}; \theta^{(j)}, \theta^{(i)}), \ \forall i, j. \tag{3}$$

However, in continual model merging, this commutative characteristic *may not hold*. Here, the ordering of models can have an impact on the final performance of the merged model. This is because, in a continual merging setting, each step of merging builds upon the previously merged model, resulting in sequential dependencies that disrupt commutativity. To illustrate, consider the continual merging process ContinualMerging (CM), where the commutative property may not hold:

$$\text{CM}\left(\text{CM}\left(\theta^{(i-1)}_{\text{merged}}; \theta^{(0)}, \theta^{(i)}\right); \theta^{(0)}, \theta^{(i+1)}\right) \stackrel{?}{=} \text{CM}\left(\text{CM}\left(\theta^{(i-1)}_{\text{merged}}; \theta^{(0)}, \theta^{(i+1)}\right); \theta^{(0)}, \theta^{(i)}\right), \ \forall i. \tag{4}$$

This non-commutative nature introduces additional complexities in the knowledge preservation of preceding models, where the quality of the final merged model hinges not just on the models themselves but critically on the ordering in which they are integrated. Moreover, *as earlier parameter information is gradually diminished throughout the sequential process, the final model might not completely encapsulate the knowledge from all individual tasks*. Consequently, it becomes essential to develop effective merging strategies that take the non-commutation property into account, balancing sequential dependencies and task knowledge retention.

Existing applications of continual model merging are prevalent in online training settings, where models are updated along the training trajectory. This approach includes techniques such as the latest weight averaging (LAWA) [34], exponential moving average (EMA) [53, 65], and stochastic weight averaging (SWA) [30]. These strategies, however, were not originally intended for scenarios with significant distribution shifts between consecutive models, which can be a critical challenge. In Dziadzio et al. [18], the authors propose the concept of temporal model merging, where they select models to merge at each step, akin to continual model merging. While most existing model merging approaches assume the simultaneous availability of expert models, research on continual model merging remains limited [43]. Some conventional model merging techniques can be revised and adapted within the framework of continual model merging. As an example, consider task arithmetic:
Baseline 3.3 (Continual Task Arithmetic). This is a straightforward extension of the conventional task arithmetic to the continual model merging scenario. The update rule can be expressed as follows:

$$\theta^{(t)}_{\text{merged}} = \theta^{(t-1)}_{\text{merged}} + \lambda(\theta^{(t)} - \theta^{(0)}), \tag{5}$$

where λ is a scalar hyperparameter that controls the contribution of the new task-specific model.

To summarize, continual model merging methods align with real-world applications where tasks emerge progressively and offer improved memory efficiency. However, it can be non-commutative, which introduces unique challenges in task knowledge retention and interference resolution.

4 Methodology

Our approach to continual model merging is motivated by three key insights: (1) *Orthogonality Preservation:* To minimize task interference, the parameter updates for new tasks should be approximately orthogonal to the existing merged parameter updates. (2) *Magnitude Control:* The magnitude

of parameter changes should remain stable throughout the merging process to prevent drift from the pre-trained model's loss basin. (3) *Information Retention:* The merged model should preserve task-specific information from all previously seen models while accommodating new tasks efficiently.

Building on these insights, we propose a projection-based continual merging approach that (1) Projects new task vectors onto subspaces orthogonal to the current merged model; (2) Employs adaptive time-varying scaling to maintain stable parameter drift from the base model; (3) Preserves task-specific information through careful parameter updates.

The complete procedure is outlined in Algorithm 1 and illustrated in Figure 3. Starting with the first task-specific model $f_{\theta^{(1)}}$, our method iteratively incorporates new models as they become available. For each new model, we handle the parameters in two distinct ways: weight matrices in linear layers undergo orthogonal projection to minimize interference, whereas other parameters, such as biases and those in non-linear layers, are averaged directly.

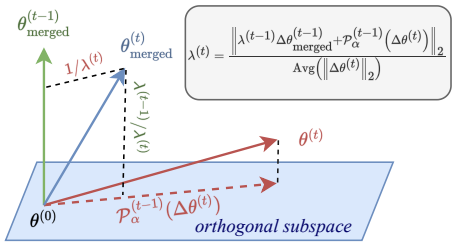

Figure 3: **Subspace view.** Geometric interpretation of the proposed continual merging approach, illustrating the orthogonal projection and adaptive scaling mechanisms.

An overview of the update rule is provided below. For weight matrices in linear layers, we propose the following update rule:

$$W^{(t)}_{\text{merged}} = W^{(0)} + \frac{\lambda^{(t-1)}\Delta W^{(t-1)}_{\text{merged}} + \mathcal{P}^{(t-1)}_{\alpha}\left(\Delta W^{(t)}\right)}{\lambda^{(t)}}, \tag{6}$$

where $W \in \mathbb{R}^{m\times n}$, $\Delta W^{(t-1)}_{\text{merged}} = W^{(t-1)}_{\text{merged}} - W^{(0)}$ and $\Delta W^{(t)} = W^{(t)} - W^{(0)}$ denote the element-wise differences between the model parameters and the pre-trained model, commonly referred to as task vectors or delta parameters [29, 100]. $\mathcal{P}^{(t-1)}_{\alpha}(\cdot)$ represents a projection mapping that projects the task vector $\Delta W^{(t)}$ onto the subspace spanned by $\Delta W^{(t-1)}_{\text{merged}}$. When a new task model (shown in solid red arrow in Figure 3) arrives, its difference from the pre-trained model $\theta^{(0)}$ is projected onto this orthogonal subspace using the projection operator $\mathcal{P}^{(t-1)}_{\alpha}$. $\lambda^{(t-1)}$ denotes a time-varying scaling factor that controls the contribution of the projected task vector to the merged model. By induction, we can expand Eq.(6) to obtain the general term formula, proved in Theorem A.1:

Algorithm 1 OPCM

Initialize $\theta^{(1)}_{\text{merged}} = \theta^{(1)}$, average norm of the task vectors $n = \|\Delta\theta^{(1)}\|_2$, scaling factor $\lambda^{(1)} = 1$.
for $t = 2$ to T **do**
  for weight matrices $W \in \mathbb{R}^{m\times n}$ in linear layers **do**
    $\Delta W^{(t-1)}_{\text{merged}} \leftarrow W^{(t-1)}_{\text{merged}} - W^{(0)}$
    $\Delta W^{(t)} \leftarrow W^{(t)} - W^{(0)}$
    $\Delta W^{(t)}_{\text{proj}} \leftarrow \mathcal{P}^{(t-1)}_{\alpha}\left(\Delta W^{(t)}; \Delta W^{(t-1)}_{\text{merged}}\right)$
  end for
  for other parameters p **do**
    $\Delta p^{(t)} \leftarrow p^{(t)} - p^{(0)}$
  end for
  $\Delta\theta^{(t-1)}_{\text{merged}} \leftarrow \theta^{(t-1)}_{\text{merged}} - \theta^{(0)}$
  Concatenate $\Delta W^{(t)}_{\text{proj}}$ and $\Delta p^{(t)}$ into $\Delta\theta^{(t)}_{\text{proj}}$
  $n \leftarrow \frac{t-1}{t}n + \frac{1}{t}\|\Delta\theta^{(t)}\|_2$
  $\lambda^{(t)} \leftarrow \left\|\lambda^{(t-1)}\Delta\theta^{(t-1)}_{\text{merged}} + \Delta\theta^{(t)}_{\text{proj}}\right\|_2 / n$
  $\theta^{(t)}_{\text{merged}} \leftarrow \theta^{(0)} + \frac{\lambda^{(t-1)}\Delta\theta^{(t-1)}_{\text{merged}} + \Delta\theta^{(t)}_{\text{proj}}}{\lambda^{(t)}}$
end for
return $\theta^{(T)}_{\text{merged}}$

$$W^{(t)}_{\text{merged}} = W^{(0)} + \frac{1}{\lambda^{(t)}}\sum_{i=1}^{t}\mathcal{P}^{(i-1)}_{\alpha}\left(\Delta W^{(i)}\right). \tag{7}$$

This formulation can be interpreted as a more generalized form of Task Arithmetic, where the task vectors are projected onto a subspace spanned by the previous merged model.

For biases in linear layers and other parameters, we simply set $\mathcal{P}^{(t-1)}_{\alpha}$ in Eq.(6) as the identity mapping. Thus the update rule is simplified as $p^{(t)}_{\text{merged}} = p^{(0)} + (\lambda^{(t-1)}\Delta p^{(t-1)}_{\text{merged}} + \Delta p^{(t)})/\lambda^{(t)}$. The general term formula degenerates to a similar form as Task Arithmetic, i.e., $p^{(t)}_{\text{merged}} = p^{(0)} + \frac{1}{\lambda^{(t)}}\sum_{i=1}^{t}\Delta p^{(i)}$.

The projection mapping $\mathcal{P}^{(t-1)}_{\alpha}$ is designed to ensure orthogonality between the incoming task vector $\Delta W^{(t)}$ and the previous merged model $\Delta W^{(t-1)}_{\text{merged}}$ while maintaining proximity between $\mathcal{P}^{(t-1)}_{\alpha}\left(\Delta W^{(t)}\right)$ and $\Delta W^{(t)}$. We first perform a full singular value decomposition (SVD) on the previous merged model $\Delta W^{(t-1)}_{\text{merged}} = U^{(t-1)}\Sigma^{(t-1)}V^{(t-1)}$, where $U^{(t-1)} \in \mathbb{R}^{m\times m}$ and $V^{(t-1)} \in$

$\mathbb{R}^{n\times n}$ comprise orthonormal basis vectors, and $\Sigma^{(t-1)} \in \mathbb{R}^{m\times n}$ is a (rectangular) diagonal matrix containing the singular values [58]. The proposed projection mapping $\mathcal{P}_\alpha^{(t-1)}$ is then defined as: $\mathcal{P}_\alpha^{(t-1)}\left(\Delta W^{(t)}\right) = \sum_{i,j=r_\alpha, i\neq j}^{m,n} \left\langle \Delta W^{(t)}, u_i v_j^T \right\rangle_F u_i v_j^T$, where u_i and v_j denote the i-th column of $U^{(t-1)}$ and the j-th column of $V^{(t-1)}$, respectively. α is the projection threshold hyper-parameter, which controls the balance between retaining existing knowledge and incorporating knowledge from new tasks. r_α represents the minimal rank of $\Delta W_{\text{merged}}^{(t-1)}$ such that $\sum_{i=1}^{r_\alpha} \sigma_i \geq \alpha \sum_{i=1}^{\min(m,n)} \sigma_i$.

The adaptive time-varying scaling factor $\lambda^{(t)}$ is introduced to maintain a consistent magnitude of the merged model's deviation from the pre-trained model throughout the merging process, specifically ensuring that the Frobenius norm $\|W_{\text{merged}}^{(t)} - W^{(0)}\|_2$ remains stable over time. The scaling factor $\lambda^{(t)}$ is computed as $\lambda^{(1)} = 1, \lambda^{(t)} = \left\|\lambda^{(t-1)}\Delta\theta_{\text{merged}}^{(t-1)} + \mathcal{P}_\alpha^{(t-1)}\left(\Delta\theta^{(t)}\right)\right\|_2 / \text{Avg}\left(\left\|\Delta\theta^{(t)}\right\|_2\right)$, where $\Delta\theta_{\text{merged}}^{(t-1)} = \theta_{\text{merged}}^{(t-1)} - \theta^{(0)}$ and $\Delta\theta^{(t)} = \theta^{(t)} - \theta^{(0)}$ represent flattened vectors of parameter differences, and $\text{Avg}(\|\Delta\theta^{(t)}\|_2) = \frac{1}{t}\sum_{i=1}^{t}\|\Delta\theta^{(i)}\|_2$ is the average norm. For notational simplicity, we apply $\mathcal{P}_\alpha^{(t-1)}$ directly to the task vector rather than to individual weight matrices.

Alternatively, the time-varying scaling factor can be set to $\lambda^{(t)} = \sqrt{t}$. This choice is motivated by empirical observations from prior work indicating that task vectors from different tasks tend to be approximately orthogonal [29, 77, 32], i.e., $\left\langle \Delta\theta^{(i)}, \Delta\theta^{(j)} \right\rangle \approx \delta_{ij}$ generally holds for all $i, j \in [1, t]$. The empirical validation of task vector orthogonality is presented in Figure 4, which analyzes 8 task-specific ViT-B/32 models. For a more comprehensive analysis across model sizes and task quantities, we present additional results in the appendix: Figure 9 (ViT-B/32), Figure 10 (ViT-B/16), and Figure 11 (ViT-L/14), each evaluated on 20 downstream tasks. This orthogonality property makes $\sqrt{t}$ a natural choice for the scaling factor, as it helps maintain the magnitude of parameter changes across merging steps.

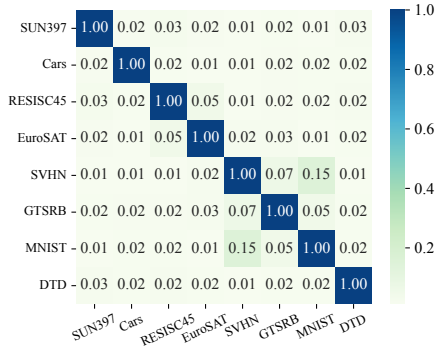

Figure 4: The cosine similarity between task vectors of ViT-B/32.

5 Theoretical Analysis

We now present some theoretical analysis of the proposed continual merging method, establishing key properties regarding orthogonality and stability. Proofs are provided in Appendix A.1 and additional discussion on the computational complexity of OPCM can be found in Appendix B.

Theorem 5.1 (Orthogonality of Projected Task Vectors)**.** *Given a sequence of task-specific models* $\{f_{\theta^{(t)}}\}_{t=1}^T$ *fine-tuned from a pre-trained model* $f_{\theta^{(0)}}$*, for any time step t, the projected task vector* $\mathcal{P}_\alpha^{(t-1)}(\Delta W^{(t)})$ *obtained from the update rule in Eq.(6) is orthogonal to* $\Delta W_{merged}^{(t-1)}$*, i.e.,*

$$\left\langle \mathcal{P}_\alpha^{(t-1)}\left(\Delta W^{(t)}\right), \Delta W_{merged}^{(t-1)} \right\rangle_F = 0. \tag{8}$$

Similar to [89], we can define the merging gap for i-th task as follows:

$$G_i = \mathcal{L}_i\left(\theta^{(0)} + \sum_{j=1}^{t}\eta_j \mathcal{P}_\alpha^{(j-1)}\left(\Delta\theta^{(i)}\right)\right) - \mathcal{L}_i\left(\theta^{(0)} + \eta_i \mathcal{P}_\alpha^{(i-1)}\left(\Delta\theta^{(i)}\right)\right). \tag{9}$$

Where $\{\eta_i\}_{i=1}^t$ is a sequence of scaling factors, and $\mathcal{L}_i$ is the loss function for i-th task. Apply Taylor expansion to G_i at $\theta^{(0)}$, we obtain the first-order approximation $G_i \approx \nabla_{\theta^{(0)}}\mathcal{L}_i^\top\left(\sum_{j=1,j\neq i}^{t}\eta_j\mathcal{P}_\alpha^{(j-1)}\left(\Delta\theta^{(i)}\right)\right)$. At time step t, we have $\eta_i = 1/\lambda^{(t)}$ for all $i \in [1, t]$. G_t is the merging gap for t-th task, which can be simplified as $G_t \approx \nabla_{\theta^{(0)}}\mathcal{L}_t^\top\left(\frac{\lambda^{(t-1)}}{\lambda^{(t)}}\Delta\theta_{\text{merged}}^{(t-1)}\right)$. On the other hand, since the task vector $\Delta\theta^{(i)}$ represents the cumulative effect of gradient updates throughout the training process, we can express the merging gap in terms of the inner product between

Table 1: The performance comparison of continual merging methods. We report the average accuracy and backward transfer (BWT) of the merged models. The best results are highlighted in bold. We abbreviate 'Continual' as 'C.' in the table to save space.

	Method	ViT-B/32			ViT-B/16			ViT-L/14		
		8 tasks	14 tasks	20 tasks	8 tasks	14 tasks	20 tasks	8 tasks	14 tasks	20 tasks
	Pre-Trained	48.1	56.9	55.6	55.4	62.0	59.8	64.9	69.1	65.6
	Fine-Tuned	90.4	89.3	89.8	92.4	91.3	91.6	94.3	93.4	93.5
	C. Fine-Tuned	79.8	67.4	62.6	82.9	72.2	68.2	90.0	70.9	77.7
ACC↑	Average (SWA)	66.3±0.0	65.4±0.0	61.1±0.0	72.3±0.0	69.7±0.0	64.8±0.0	80.0±0.0	77.5±0.0	71.1±0.0
ACC↑	C. Task Arithmetic	67.5±0.0	66.5±0.0	60.6±0.0	77.1±0.0	70.9±0.0	64.2±0.0	82.1±0.0	77.9±0.0	70.3±0.0
ACC↑	C. Ties-Merging	49.0±10.2	66.2±0.6	59.9±0.7	66.8±3.7	70.5±0.8	63.0±1.6	64.3±7.0	78.0±0.6	68.3±0.9
ACC↑	**OPCM (Ours)**	**75.5**±0.5	**71.9**±0.3	**65.7**±0.2	**81.8**±0.3	**77.1**±0.5	**70.3**±0.2	**87.0**±0.4	**83.5**±0.2	**76.0**±0.2
BWT↑	Average (SWA)	-11.5±2.2	-8.0±1.3	-7.1±2.1	-9.7±1.5	-7.1±1.4	-7.3±1.7	-7.3±1.4	-5.8±1.0	-6.4±1.5
BWT↑	C. Task Arithmetic	-9.6±1.5	-1.3±0.3	-3.4±0.4	**-4.2**±1.0	-1.3±0.4	-3.6±0.4	-7.1±0.8	-1.8±0.3	-3.3±0.3
BWT↑	C. Ties-Merging	-15.3±8.0	**1.9**±0.6	**-1.5**±0.7	-5.5±0.4	**1.4**±0.7	**-1.5**±1.2	-13.0±5.7	**1.1**±0.4	**-2.9**±1.0
BWT↑	**OPCM (Ours)**	**-6.3**±1.1	-6.0±1.0	-7.8±1.5	-4.8±0.7	-5.1±1.4	-6.3±2.2	**-2.6**±1.0	-4.3±0.7	-6.5±1.8

task vectors as $G_t \approx C\Delta\theta^{(t)\top}\Delta\theta^{(t-1)}_{\text{merged}}$, where C is a constant [77, 89]. Consequently, enforcing orthogonality between these vectors ($\Delta\theta^{(t)\top}\Delta\theta^{(t-1)}_{\text{merged}} = 0$) serves to minimize the gap G_t.

Theorem 5.2 (Bounded Parameter Distance)**.** *Under the update rule in Eq.(6) with the empirical choice of scaling factor $\lambda^{(t)} = \sqrt{t}$, the distance between the merged model and the pre-trained model remains bounded:*

$$\left\| W^{(t)}_{merged} - W^{(0)} \right\|_F^2 \leq \max_{i\in[1,t]} \left\| \Delta W^{(i)} \right\|_F^2 . \tag{10}$$

The proposed continual merging method ensures that the merged model maintains a stable distance from the pre-trained model throughout the merging process, preventing parameter drift that could lead to catastrophic forgetting.

Corollary 5.3 (Preservation of Task Information)**.** *For any time step t, the merged model preserves information from all previous tasks in the following sense:*

$$W^{(t)}_{merged} - W^{(0)} = \frac{1}{\lambda^{(t)}} \sum_{i=1}^{t} \mathcal{P}^{(i-1)}_{\alpha} \left(\Delta W^{(i)} \right). \tag{11}$$

This formulation follows directly from Eq.(7). This corollary demonstrates that our continual merging approach maintains a weighted combination of all previously learned task-specific changes, where each task's contribution is preserved through its projection. In Appendix A.2, we further discuss the special case where two adjacent task vectors are highly correlated, and our method can automatically filter redundant knowledge in the incoming task vector.

6 Experiments

In this section, we present the experimental results of our continual merging approach and the ablation studies for a comprehensive analysis of our method.

Experimental Setup: (1) *Models and datasets*. We first fine-tune the CLIP-ViT models [63] on up to 20 downstream tasks. Following [83], we evaluate our approach on three task sets of increasing size: a base set of 8 tasks, an extended set of 14 tasks, and the complete set of 20 tasks. This hierarchical grouping allows us to analyze how our method scales with increasing task diversity and complexity. Additional experimental details are provided in Appendix C. (2) *Evaluation metrics*. To evaluate our merged models, we employ two key metrics: average accuracy (ACC) and backward transfer (BWT) [45], details are provided in Appendix D.2.

6.1 Continual Multi-Task Model Merging

We evaluate our method on three different CLIP-ViT architectures (ViT-B/32, ViT-B/16, and ViT-L/14) across three task sets of increasing size (8, 14, and 20 tasks). For each experiment, we set $\alpha = 0.5$ and repeat the experiment 10 times with shuffled task order and report the mean and standard deviation of the results. We compare our continual merging approach against four baselines: (1) Continual fine-tuning, (2) Simple Weight Averaging (SWA), which takes the arithmetic mean of model parameters, (3) Continual Task Arithmetic [29], which performs weighted averaging based on task-specific scaling factors, and (4) Continual Ties-Merging [91]. Details are in Appendix D.3.1.

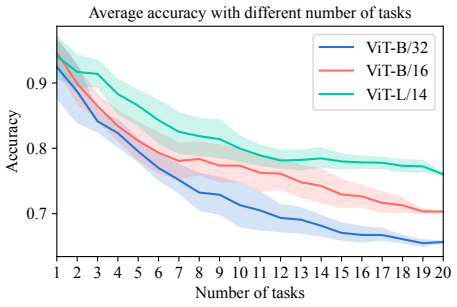

Figure 5: Performance comparison of ViT models with different architectures across an increasing number of sequential tasks.

As shown in Table 1, our method consistently outperforms the baseline methods across all model architectures and task sets. Our method consistently achieves improvements of 5-8% over continual Task Arithmetic and continual Ties-Merging. In addition, the performance gain is maintained as we scale the task set size and model capacity. Furthermore, the backward transfer (BWT) results demonstrate our method's ability to retain knowledge of previously learned tasks. While some negative transfer is inevitable in a continual learning setting, our approach shows better BWT scores compared to the baselines in most cases. The larger ViT-L/14 model exhibits the least forgetting, with a BWT of only -2.6% on the 8-task set, suggesting that increased model capacity helps mitigate catastrophic forgetting.

In Figure 5, we show a line plot comparing the average accuracy of three different Vision Transformer (ViT) architectures as they handle an increasing number of tasks from 1 to 20 ($\alpha = 0.5$). For each run, the order of the tasks is shuffled. Each line represents a different model variant, with shaded areas indicating confidence intervals. The plot demonstrates a general downward trend in accuracy as more tasks are added, with ViT-L/14 maintaining the highest performance throughout. Starting from around 90% accuracy for all models, there's a gradual decline, with ViT-L/14 maintaining approximately 75-80% accuracy by task 20, while the smaller models (ViT-B/32 and ViT-B/16) show steeper degradation, dropping to around 65-70% accuracy.

(1) *Robustness to task ordering.* The relatively narrow confidence bands in Figure 5 and small standard deviations in Table 1 demonstrate that our method is robust to different task orderings, maintaining consistent overall performance regardless of the sequence in which tasks are presented. Even as the number of tasks increases to 20, the performance variation remains contained, suggesting that our orthogonal projection mechanism effectively manages task interference regardless of the order in which tasks are merged. This robustness to task order is a crucial practical advantage of a continual merging technique, as it eliminates the need for careful task sequence engineering in real-world applications. (2) *Model size matters in average performance.* We also observe that model size plays a crucial role in the merging performance. The ViT-L/14 consistently achieves better results than ViT-B/32 and ViT-B/16, this indicates that larger models may be better suited for continual multi-task merging, possibly due to their increased dimensionality, which helps manage parameter interference by expanding the orthogonal subspace where task-specific updates can exist without affecting other tasks. This property is particularly beneficial when merging multiple task-specific models. (3) *Model size matters in mitigating forgetting.* The results in Table 1 and Figure 5 also indicate that model size plays a crucial role in mitigating catastrophic forgetting during continual merging. While all models show some degree of performance degradation as the number of tasks increases, the rate of decline varies significantly with model capacity. The ViT-L/14, our largest model, exhibits the most graceful degradation (-17.5% drops at 20 tasks compared to individuals). In contrast, the smaller ViT-B/32 and ViT-B/16 models show steeper performance drops (24.1% and 21.3% average accuracy drops at 20 tasks, respectively).

6.2 Hyper-Parameter Analysis

Ablations on the projection threshold α. We perform ablation studies on the projection threshold α to validate the robustness of proposed method to different hyper-parameter settings. Figure 6 presents a comparative ablation study between Task Arithmetic (a) and our method (b) on ViT-B/32 across

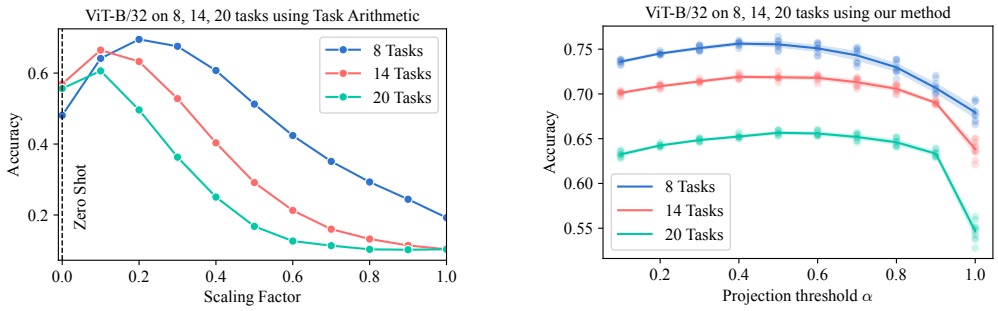

(a) Task Arithmetic (b) OPCM (Ours)

Figure 6: Ablations on the hyper-parameter settings. We compare our method with Task Arithmetic. This figure highlights the robustness of our method to different hyper-parameter settings.

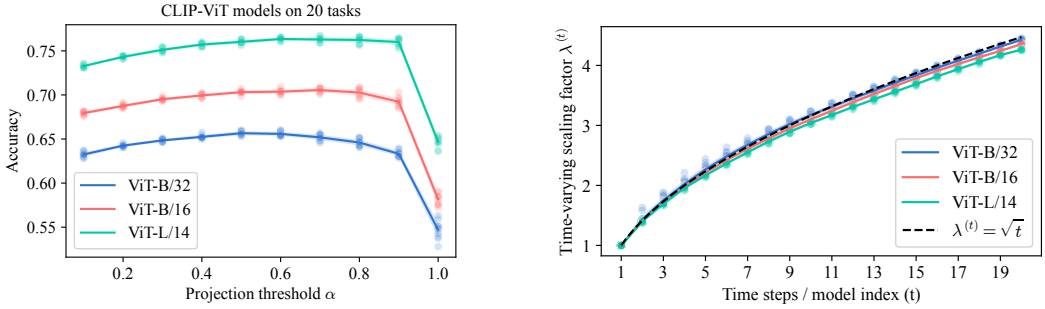

(a) (b)

Figure 7: Hyper-parameters analysis. (a) Performance comparison with varying size of models across different projection threshold on 20 tasks; (b) The adaptive scaling factor $\lambda^{(t)}$ across different steps.

different task scales. Several key findings emerge from this comparison: (1) *Knowledge retention and new task learning trade-off*. Across all task sets, the performance curves exhibit a consistent inverted U-shape pattern, with optimal performance achieved in the range of $\alpha \approx 0.4 - 0.6$. This suggests that moderate projection thresholds strike an optimal balance between preserving task-specific information and managing interference between tasks. (2) *Hyperparameter robustness and transferability*. Our method demonstrates remarkably more stable performance across hyperparameter ranges compared to Task Arithmetic. The optimal α value remains relatively consistent ($\approx$0.5) regardless of the number of tasks, demonstrating the robustness and transferability across different configurations. This stability and transferability is particularly valuable from a practical perspective especially when hyper-parameter tuning is expensive, thus minimal tuning of α is required when scaling to different numbers of tasks. In Figure 7a we also show the performance comparison of CLIP-ViT models of different sizes with varying α on 20 tasks. It is observed that all three models show stable performance and similar trends as the projection threshold changes. More details are provided in Appendix D.4.

Empirical analysis of the adaptive time-varying scaling factor $\lambda^{(t)}$. In our method, the scaling factor $\lambda^{(t)}$ is adaptively adjusted based on the norm ratio between the combined task vectors and the average task vector norm. This adaptive mechanism helps maintain stable parameter distances throughout the merging process. Figure 7b shows the adaptive scaling factor $\lambda^{(t)}$ across different steps. The adaptive scaling factors closely follow a $\sqrt{t}$ curve (shown as the dashed black line), empirically validating our hypothesis of an empirical choice of $\lambda^{(t)} = \sqrt{t}$ in Section 4. All three model architectures (ViT-B/32, ViT-B/16, and ViT-L/14) exhibit remarkably similar scaling patterns, indicating that this time-varying adaptive scaling mechanism is also robust and transferable across different model capacities.

7 Conclusion and Future Work

In this work, we presented a novel training-free projection-based continual model merging method for combining multiple fine-tuned models *sequentially*. Our approach addresses several key challenges in model merging through orthogonal projections of weight matrices and adaptive scaling mechanisms.

Through extensive experiments, we demonstrated that our method consistently outperforms baseline approaches. The results show that our approach achieves 5-8% average accuracy improvement while maintaining robust performance across different task orderings. The effectiveness of our method scales well with model capacity, with larger models showing a better ability to mitigate catastrophic forgetting during sequential merging.

While our current work focuses on vision models, the proposed method's principles are generally applicable to other domains. Future work could explore extensions to language models, multi-modal architectures, and other scenarios where sequential model merging is beneficial. Additionally, investigating the relationship between model capacity and merging performance could provide valuable insights.

Broader impacts

This research advances the field of model merging with potential positive impacts on computational efficiency and accessibility of machine learning systems. By enabling effective continual merging of task-specific models, our method can significantly reduce storage requirements and computational costs associated with maintaining multiple specialized models. This efficiency gain could lead to reduced energy consumption and carbon footprint in AI deployments.

Acknowledgments and Disclosure of Funding

This work is supported by the National Natural Science Foundation of China (Grant No. 62225113, U23A20318, U2336211, 62576364 and 62276195), the Foundation for Innovative Research Groups of Hubei Province (Grant No. 2024AFA017), the Science and Technology Major Project of Hubei Province (Grant No. 2024BAB046) and the Shenzhen Basic Research Project (Natural Science Foundation) Basic Research Key Project (NO. JCYJ20241202124430041). Dr. Tao's research is partially supported by NTU RSR and Start Up Grants. The numerical calculations in this paper have been done on the supercomputing system in the Supercomputing Center of Wuhan University.

References

[1] Arash Ahmadian, Seraphina Goldfarb-Tarrant, Beyza Ermis, Marzieh Fadaee, Sara Hooker, et al. Mix data or merge models? optimizing for diverse multi-task learning. *arXiv preprint arXiv:2410.10801*, 2024.

[2] Samuel Ainsworth, Jonathan Hayase, and Siddhartha Srinivasa. Git re-basin: Merging models modulo permutation symmetries. In *The Eleventh International Conference on Learning Representations*, 2023.

[3] Devansh Arpit, Huan Wang, Yingbo Zhou, and Caiming Xiong. Ensemble of averages: Improving model selection and boosting performance in domain generalization. *Advances in Neural Information Processing Systems*, 35:8265–8277, 2022.

[4] Lukas Bossard, Matthieu Guillaumin, and Luc Van Gool. Food-101–mining discriminative components with random forests. In *Computer vision–ECCV 2014: 13th European conference, zurich, Switzerland, September 6-12, 2014, proceedings, part VI 13*, pages 446–461. Springer, 2014.

[5] Pietro Buzzega, Matteo Boschini, Angelo Porrello, Davide Abati, and Simone Calderara. Dark experience for general continual learning: a strong, simple baseline. *Advances in neural information processing systems*, 33:15920–15930, 2020.

[6] Arslan Chaudhry, Ranzato Marc'Aurelio, Marcus Rohrbach, and Mohamed Elhoseiny. Efficient lifelong learning with a-gem. In *7th International Conference on Learning Representations, ICLR 2019*. International Conference on Learning Representations, ICLR, 2019.

[7] Atoosa Chegini, Hamid Kazemi, Seyed Iman Mirzadeh, Dong Yin, Maxwell Horton, Moin Nabi, Mehrdad Farajtabar, and Keivan Alizadeh. Model soup for better rlhf: Weight space averaging to improve alignment in llms. In *NeurIPS 2024 Workshop on Fine-Tuning in Modern Machine Learning: Principles and Scalability*, 2024.

[8] Chi Chen, Yiyang Du, Zheng Fang, Ziyue Wang, Fuwen Luo, Peng Li, Ming Yan, Ji Zhang, Fei Huang, Maosong Sun, et al. Model composition for multimodal large language models. In *Proceedings of the 62nd Annual Meeting of the Association for Computational Linguistics (Volume 1: Long Papers)*, pages 11246–11262, 2024.

[9] Weiyu Chen and James Kwok. You only merge once: Learning the pareto set of preference-aware model merging. *arXiv preprint arXiv:2408.12105*, 2024.

[10] Gong Cheng, Junwei Han, and Xiaoqiang Lu. Remote sensing image scene classification: Benchmark and state of the art. *Proceedings of the IEEE*, 105(10):1865–1883, 2017.

[11] Mircea Cimpoi, Subhransu Maji, Iasonas Kokkinos, Sammy Mohamed, and Andrea Vedaldi. Describing textures in the wild. In *Proceedings of the IEEE conference on computer vision and pattern recognition*, pages 3606–3613, 2014.

[12] Tarin Clanuwat, Mikel Bober-Irizar, Asanobu Kitamoto, Alex Lamb, Kazuaki Yamamoto, and David Ha. Deep learning for classical japanese literature. *arXiv preprint arXiv:1812.01718*, 2018.

[13] Adam Coates, Andrew Ng, and Honglak Lee. An analysis of single-layer networks in unsupervised feature learning. In *Proceedings of the fourteenth international conference on artificial intelligence and statistics*, pages 215–223. JMLR Workshop and Conference Proceedings, 2011.

[14] Gregory Cohen, Saeed Afshar, Jonathan Tapson, and Andre Van Schaik. Emnist: Extending mnist to handwritten letters. In *2017 international joint conference on neural networks (IJCNN)*, pages 2921–2926. IEEE, 2017.

[15] Nikolaos Dimitriadis, Pascal Frossard, and Francois Fleuret. Pareto low-rank adapters: Efficient multi-task learning with preferences. *arXiv preprint arXiv:2407.08056*, 2024.

[16] Thang Doan, Mehdi Abbana Bennani, Bogdan Mazoure, Guillaume Rabusseau, and Pierre Alquier. A theoretical analysis of catastrophic forgetting through the ntk overlap matrix. In *International Conference on Artificial Intelligence and Statistics*, pages 1072–1080. PMLR, 2021.

[17] Felix Draxler, Kambis Veschgini, Manfred Salmhofer, and Fred Hamprecht. Essentially no barriers in neural network energy landscape. In *International conference on machine learning*, pages 1309–1318. PMLR, 2018.

[18] Sebastian Dziadzio, Vishaal Udandarao, Karsten Roth, Ameya Prabhu, Zeynep Akata, Samuel Albanie, and Matthias Bethge. How to merge your multimodal models over time? *arXiv preprint arXiv:2412.06712*, 2024.

[19] Mehrdad Farajtabar, Navid Azizan, Alex Mott, and Ang Li. Orthogonal gradient descent for continual learning. In *International Conference on Artificial Intelligence and Statistics*, pages 3762–3773. PMLR, 2020.

[20] Chrisantha Fernando, Dylan Banarse, Charles Blundell, Yori Zwols, David Ha, Andrei A Rusu, Alexander Pritzel, and Daan Wierstra. Pathnet: Evolution channels gradient descent in super neural networks. *arXiv preprint arXiv:1701.08734*, 2017.

[21] Jonathan Frankle, Gintare Karolina Dziugaite, Daniel Roy, and Michael Carbin. Linear mode connectivity and the lottery ticket hypothesis. In *International Conference on Machine Learning*, pages 3259–3269. PMLR, 2020.

[22] C Daniel Freeman and Joan Bruna. Topology and geometry of half-rectified network optimization. In *International Conference on Learning Representations*, 2017.

[23] Antonio Andrea Gargiulo, Donato Crisostomi, Maria Sofia Bucarelli, Simone Scardapane, Fabrizio Silvestri, and Emanuele Rodola. Task singular vectors: Reducing task interference in model merging. In *Proceedings of the Computer Vision and Pattern Recognition Conference*, pages 18695–18705, 2025.

[24] Ian J Goodfellow, Dumitru Erhan, Pierre Luc Carrier, Aaron Courville, Mehdi Mirza, Ben Hamner, Will Cukierski, Yichuan Tang, David Thaler, Dong-Hyun Lee, et al. Challenges in representation learning: A report on three machine learning contests. In *Neural information processing: 20th international conference, ICONIP 2013, daegu, korea, november 3-7, 2013. Proceedings, Part III 20*, pages 117–124. Springer, 2013.

[25] Alexey Gorbatovski, Boris Shaposhnikov, Alexey Malakhov, Nikita Surnachev, Yaroslav Aksenov, Ian Maksimov, Nikita Balagansky, and Daniil Gavrilov. Learn your reference model for real good alignment. In *The Thirteenth International Conference on Learning Representations*, 2025.

[26] Patrick Helber, Benjamin Bischke, Andreas Dengel, and Damian Borth. Eurosat: A novel dataset and deep learning benchmark for land use and land cover classification. *IEEE Journal of Selected Topics in Applied Earth Observations and Remote Sensing*, 12(7):2217–2226, 2019.

[27] Yongqi Huang, Peng Ye, Xiaoshui Huang, Sheng Li, Tao Chen, Tong He, and Wanli Ouyang. Experts weights averaging: A new general training scheme for vision transformers. *arXiv preprint arXiv:2308.06093*, 2023.

[28] Gabriel Ilharco, Mitchell Wortsman, Samir Yitzhak Gadre, Shuran Song, Hannaneh Hajishirzi, Simon Kornblith, Ali Farhadi, and Ludwig Schmidt. Patching open-vocabulary models by interpolating weights. *Advances in Neural Information Processing Systems*, 35:29262–29277, 2022.

[29] Gabriel Ilharco, Marco Tulio Ribeiro, Mitchell Wortsman, Ludwig Schmidt, Hannaneh Hajishirzi, and Ali Farhadi. Editing models with task arithmetic. In *The Eleventh International Conference on Learning Representations*, 2023.

[30] Pavel Izmailov, Dmitrii Podoprikhin, Timur Garipov, Dmitry Vetrov, and Andrew Gordon Wilson. Averaging weights leads to wider optima and better generalization. In *34th Conference on Uncertainty in Artificial Intelligence 2018, UAI 2018*, pages 876–885. Association For Uncertainty in Artificial Intelligence (AUAI), 2018.

[31] Junguang Jiang, Baixu Chen, Junwei Pan, Ximei Wang, Dapeng Liu, Jie Jiang, and Mingsheng Long. Forkmerge: Mitigating negative transfer in auxiliary-task learning. *Advances in Neural Information Processing Systems*, 36, 2024.

[32] Ruochen Jin, Bojian Hou, Jiancong Xiao, Weijie Su, and Li Shen. Fine-tuning linear layers only is a simple yet effective way for task arithmetic. *arXiv preprint arXiv:2407.07089*, 2024.

[33] Xisen Jin, Xiang Ren, Daniel Preotiuc-Pietro, and Pengxiang Cheng. Dataless knowledge fusion by merging weights of language models. In *The Eleventh International Conference on Learning Representations*, 2023.

[34] Jean Kaddour. Stop wasting my time! saving days of imagenet and bert training with latest weight averaging. *arXiv preprint arXiv:2209.14981*, 2022.

[35] Arham Khan, Todd Nief, Nathaniel Hudson, Mansi Sakarvadia, Daniel Grzenda, Aswathy Ajith, Jordan Pettyjohn, Kyle Chard, and Ian Foster. Sok: On finding common ground in loss landscapes using deep model merging techniques. *arXiv preprint arXiv:2410.12927*, 2024.

[36] Edan Kinderman, Itay Hubara, Haggai Maron, and Daniel Soudry. Foldable supernets: Scalable merging of transformers with different initializations and tasks. *arXiv preprint arXiv:2410.01483*, 2024.

[37] James Kirkpatrick, Razvan Pascanu, Neil Rabinowitz, Joel Veness, Guillaume Desjardins, Andrei A Rusu, Kieran Milan, John Quan, Tiago Ramalho, Agnieszka Grabska-Barwinska, et al. Overcoming catastrophic forgetting in neural networks. *Proceedings of the national academy of sciences*, 114(13): 3521–3526, 2017.

[38] Aran Komatsuzaki, Joan Puigcerver, James Lee-Thorp, Carlos Riquelme Ruiz, Basil Mustafa, Joshua Ainslie, Yi Tay, Mostafa Dehghani, and Neil Houlsby. Sparse upcycling: Training mixture-of-experts from dense checkpoints. In *The Eleventh International Conference on Learning Representations*.

[39] Jonathan Krause, Michael Stark, Jia Deng, and Li Fei-Fei. 3d object representations for fine-grained categorization. In *Proceedings of the IEEE international conference on computer vision workshops*, pages 554–561, 2013.

[40] Alex Krizhevsky, Geoffrey Hinton, et al. Learning multiple layers of features from tiny images. 2009.

[41] Yann LeCun, Léon Bottou, Yoshua Bengio, and Patrick Haffner. Gradient-based learning applied to document recognition. *Proceedings of the IEEE*, 86(11):2278–2324, 1998.

[42] Tao Li, Weisen Jiang, Fanghui Liu, Xiaolin Huang, and James T Kwok. Learning scalable model soup on a single gpu: An efficient subspace training strategy. In *European Conference on Computer Vision*, pages 342–359. Springer, 2024.

[43] Weishi Li, Yong Peng, Miao Zhang, Liang Ding, Han Hu, and Li Shen. Deep model fusion: A survey, 2023.

[44] Zexi Li, Zhiqi Li, Jie Lin, Tao Shen, Tao Lin, and Chao Wu. Training-time neuron alignment through permutation subspace for improving linear mode connectivity and model fusion. *arXiv preprint arXiv:2402.01342*, 2024.

[45] Sen Lin, Li Yang, Deliang Fan, and Junshan Zhang. Beyond not-forgetting: Continual learning with backward knowledge transfer. *Advances in Neural Information Processing Systems*, 35:16165–16177, 2022.

[46] Yong Lin, Hangyu Lin, Wei Xiong, Shizhe Diao, Jianmeng Liu, Jipeng Zhang, Rui Pan, Haoxiang Wang, Wenbin Hu, Hanning Zhang, et al. Mitigating the alignment tax of rlhf. In *Proceedings of the 2024 Conference on Empirical Methods in Natural Language Processing*, pages 580–606, 2024.

[47] Chang Liu, Chenfei Lou, Runzhong Wang, Alan Yuhan Xi, Li Shen, and Junchi Yan. Deep neural network fusion via graph matching with applications to model ensemble and federated learning. In *International Conference on Machine Learning*, pages 13857–13869. PMLR, 2022.

[48] Tian Yu Liu and Stefano Soatto. Tangent model composition for ensembling and continual fine-tuning. In *Proceedings of the IEEE/CVF International Conference on Computer Vision*, pages 18676–18686, 2023.

[49] David Lopez-Paz and Marc'Aurelio Ranzato. Gradient episodic memory for continual learning. *Advances in neural information processing systems*, 30, 2017.

[50] Jinliang Lu, Ziliang Pang, Min Xiao, Yaochen Zhu, Rui Xia, and Jiajun Zhang. Merge, ensemble, and cooperate! a survey on collaborative strategies in the era of large language models. *arXiv preprint arXiv:2407.06089*, 2024.

[51] Zhenyi Lu, Chenghao Fan, Wei Wei, Xiaoye Qu, Dangyang Chen, and Yu Cheng. Twin-merging: Dynamic integration of modular expertise in model merging. *arXiv preprint arXiv:2406.15479*, 2024.

[52] Michael S Matena and Colin A Raffel. Merging models with fisher-weighted averaging. *Advances in Neural Information Processing Systems*, 35:17703–17716, 2022.

[53] Daniel Morales-Brotons, Thijs Vogels, and Hadrien Hendrikx. Exponential moving average of weights in deep learning: Dynamics and benefits. *Transactions on Machine Learning Research*, 2024.

[54] Anshul Nasery, Jonathan Hayase, Pang Wei Koh, and Sewoong Oh. Pleas–merging models with permutations and least squares. *arXiv preprint arXiv:2407.02447*, 2024.

[55] Yuval Netzer, Tao Wang, Adam Coates, Alessandro Bissacco, Baolin Wu, Andrew Y Ng, et al. Reading digits in natural images with unsupervised feature learning. In *NIPS workshop on deep learning and unsupervised feature learning*, volume 2011, page 4. Granada, 2011.

[56] Cuong V Nguyen, Yingzhen Li, Thang D Bui, and Richard E Turner. Variational continual learning. *arXiv preprint arXiv:1710.10628*, 2017.

[57] Maria-Elena Nilsback and Andrew Zisserman. Automated flower classification over a large number of classes. In *2008 Sixth Indian conference on computer vision, graphics & image processing*, pages 722–729. IEEE, 2008.

[58] Peter J. Olver and Chehrzad Shakiban. *Applied Linear Algebra*. Undergraduate Texts in Mathematics. Springer International Publishing, Cham, 2018. ISBN 978-3-319-91040-6 978-3-319-91041-3. doi: 10.1007/978-3-319-91041-3. URL `http://link.springer.com/10.1007/978-3-319-91041-3`.

[59] Guillermo Ortiz-Jimenez, Alessandro Favero, and Pascal Frossard. Task arithmetic in the tangent space: Improved editing of pre-trained models. *Advances in Neural Information Processing Systems*, 36, 2024.

[60] Omkar M Parkhi, Andrea Vedaldi, Andrew Zisserman, and CV Jawahar. Cats and dogs. In *2012 IEEE conference on computer vision and pattern recognition*, pages 3498–3505. IEEE, 2012.

[61] Shiva Kumar Pentyala, Zhichao Wang, Bin Bi, Kiran Ramnath, Xiang-Bo Mao, Regunathan Radhakrishnan, Sitaram Asur, Na, and Cheng. Paft: A parallel training paradigm for effective llm fine-tuning. *arXiv preprint arXiv:2406.17923*, 2024. URL `https://arxiv.org/abs/2406.17923`.

[62] Akshara Prabhakar, Yuanzhi Li, Karthik Narasimhan, Sham Kakade, Eran Malach, and Samy Jelassi. Lora soups: Merging loras for practical skill composition tasks. In *Proceedings of the 31st International Conference on Computational Linguistics: Industry Track*, pages 644–655, 2025.

[63] Alec Radford, Jong Wook Kim, Chris Hallacy, Aditya Ramesh, Gabriel Goh, Sandhini Agarwal, Girish Sastry, Amanda Askell, Pamela Mishkin, Jack Clark, et al. Learning transferable visual models from natural language supervision. In *International conference on machine learning*, pages 8748–8763. PMLR, 2021.

[64] Alexandre Rame, Guillaume Couairon, Corentin Dancette, Jean-Baptiste Gaya, Mustafa Shukor, Laure Soulier, and Matthieu Cord. Rewarded soups: towards pareto-optimal alignment by interpolating weights fine-tuned on diverse rewards. *Advances in Neural Information Processing Systems*, 36, 2024.

[65] Karsten Roth, Vishaal Udandarao, Sebastian Dziadzio, Ameya Prabhu, Mehdi Cherti, Oriol Vinyals, Olivier Hénaff, Samuel Albanie, Matthias Bethge, and Zeynep Akata. A practitioner's guide to continual multimodal pretraining. *arXiv preprint arXiv:2408.14471*, 2024.

[66] Andrei A Rusu, Neil C Rabinowitz, Guillaume Desjardins, Hubert Soyer, James Kirkpatrick, Koray Kavukcuoglu, Razvan Pascanu, and Raia Hadsell. Progressive neural networks. *arXiv preprint arXiv:1606.04671*, 2016.

[67] Ildus Sadrtdinov, Dmitrii Pozdeev, Dmitry P Vetrov, and Ekaterina Lobacheva. To stay or not to stay in the pre-train basin: Insights on ensembling in transfer learning. *Advances in Neural Information Processing Systems*, 36, 2024.

[68] Omer Sagi and Lior Rokach. Ensemble learning: A survey. *Wiley interdisciplinary reviews: data mining and knowledge discovery*, 8(4):e1249, 2018.

[69] Li Shen, Anke Tang, Enneng Yang, Guibing Guo, Yong Luo, Lefei Zhang, Xiaochun Cao, Bo Du, and Dacheng Tao. Efficient and effective weight-ensembling mixture of experts for multi-task model merging. *arXiv preprint arXiv:2410.21804*, 2024.

[70] Richard Socher, Alex Perelygin, Jean Wu, Jason Chuang, Christopher D Manning, Andrew Y Ng, and Christopher Potts. Recursive deep models for semantic compositionality over a sentiment treebank. In *Proceedings of the 2013 conference on empirical methods in natural language processing*, pages 1631–1642, 2013.

[71] Johannes Stallkamp, Marc Schlipsing, Jan Salmen, and Christian Igel. Man vs. computer: Benchmarking machine learning algorithms for traffic sign recognition. *Neural networks*, 32:323–332, 2012.

[72] G Stoica, D Bolya, J Bjorner, P Ramesh, T Hearn, and J Hoffman. Zipit! merging models from different tasks without training. In *International Conference on Learning Representations*. International Conference on Learning Representations, 2024.

[73] Derek Tam, Mohit Bansal, and Colin Raffel. Merging by matching models in task parameter subspaces. *Transactions on Machine Learning Research*, 2024.

[74] Anke Tang, Li Shen, Yong Luo, Liang Ding, Han Hu, Bo Du, and Dacheng Tao. Concrete subspace learning based interference elimination for multi-task model fusion. *arXiv preprint arXiv:2312.06173*, 2023.

[75] Anke Tang, Li Shen, Yong Luo, Han Hu, Bo Do, and Dacheng Tao. Fusionbench: A comprehensive benchmark of deep model fusion. *arXiv preprint arXiv:2406.03280*, 2024.

[76] Anke Tang, Li Shen, Yong Luo, Shiwei Liu, Han Hu, and Bo Du. Towards efficient pareto set approximation via mixture of experts based model fusion. *arXiv preprint arXiv:2406.09770*, 2024.

[77] Anke Tang, Li Shen, Yong Luo, Yibing Zhan, Han Hu, Bo Du, Yixin Chen, and Dacheng Tao. Parameter-efficient multi-task model fusion with partial linearization. In *The Twelfth International Conference on Learning Representations*, 2024.

[78] Zhixu Tao, Ian Mason, Sanjeev Kulkarni, and Xavier Boix. Task arithmetic through the lens of one-shot federated learning. *arXiv preprint arXiv:2411.18607*, 2024.

[79] Selim Furkan Tekin, Fatih Ilhan, Tiansheng Huang, Sihao Hu, Zachary Yahn, and Ling Liu. H3 fusion: Helpful, harmless, honest fusion of aligned llms. *arXiv preprint arXiv:2411.17792*, 2024.

[80] Bastiaan S Veeling, Jasper Linmans, Jim Winkens, Taco Cohen, and Max Welling. Rotation equivariant cnns for digital pathology. In *Medical Image Computing and Computer Assisted Intervention–MICCAI 2018: 21st International Conference, Granada, Spain, September 16-20, 2018, Proceedings, Part II 11*, pages 210–218. Springer, 2018.

[81] Fanqi Wan, Xinting Huang, Deng Cai, Xiaojun Quan, Wei Bi, and Shuming Shi. Knowledge fusion of large language models. In *The Twelfth International Conference on Learning Representations*, 2024.

[82] Hu Wang, Congbo Ma, Ibrahim Almakky, Ian Reid, Gustavo Carneiro, and Mohammad Yaqub. Rethinking weight-averaged model-merging. *arXiv preprint arXiv:2411.09263*, 2024.

[83] Ke Wang, Nikolaos Dimitriadis, Guillermo Ortiz-Jimenez, François Fleuret, and Pascal Frossard. Localizing task information for improved model merging and compression. *arXiv preprint arXiv:2405.07813*, 2024.

[84] Zhenyi Wang, Enneng Yang, Li Shen, and Heng Huang. A comprehensive survey of forgetting in deep learning beyond continual learning. *IEEE Transactions on Pattern Analysis and Machine Intelligence*, 2024.

[85] Thomas Wolf, Lysandre Debut, Victor Sanh, Julien Chaumond, Clement Delangue, Anthony Moi, Pierric Cistac, Tim Rault, Rémi Louf, Morgan Funtowicz, et al. Huggingface's transformers: State-of-the-art natural language processing. *arXiv preprint arXiv:1910.03771*, 2019.

[86] Mitchell Wortsman, Gabriel Ilharco, Samir Ya Gadre, Rebecca Roelofs, Raphael Gontijo-Lopes, Ari S Morcos, Hongseok Namkoong, Ali Farhadi, Yair Carmon, Simon Kornblith, et al. Model soups: averaging weights of multiple fine-tuned models improves accuracy without increasing inference time. In *International conference on machine learning*, pages 23965–23998. PMLR, 2022.

[87] Han Xiao, Kashif Rasul, and Roland Vollgraf. Fashion-mnist: a novel image dataset for benchmarking machine learning algorithms. *arXiv preprint arXiv:1708.07747*, 2017.

[88] Jianxiong Xiao, James Hays, Krista A Ehinger, Aude Oliva, and Antonio Torralba. Sun database: Large-scale scene recognition from abbey to zoo. In *2010 IEEE computer society conference on computer vision and pattern recognition*, pages 3485–3492. IEEE, 2010.

[89] Feng Xiong, Runxi Cheng, Wang Chen, Zhanqiu Zhang, Yiwen Guo, Chun Yuan, and Ruifeng Xu. Multi-task model merging via adaptive weight disentanglement. *arXiv preprint arXiv:2411.18729*, 2024.

[90] Yichu Xu, Xin-Chun Li, Le Gan, and De-Chuan Zhan. Weight scope alignment: A frustratingly easy method for model merging. In *ECAI 2024*, pages 1720–1727. IOS Press, 2024.

[91] Prateek Yadav, Derek Tam, Leshem Choshen, Colin A Raffel, and Mohit Bansal. Ties-merging: Resolving interference when merging models. *Advances in Neural Information Processing Systems*, 36:7093–7115, 2023.

[92] Prateek Yadav, Colin Raffel, Mohammed Muqeeth, Lucas Caccia, Haokun Liu, Tianlong Chen, Mohit Bansal, Leshem Choshen, and Alessandro Sordoni. A survey on model moerging: Recycling and routing among specialized experts for collaborative learning. *arXiv preprint arXiv:2408.07057*, 2024.

[93] Prateek Yadav, Tu Vu, Jonathan Lai, Alexandra Chronopoulou, Manaal Faruqui, Mohit Bansal, and Tsendsuren Munkhdalai. What matters for model merging at scale? *arXiv preprint arXiv:2410.03617*, 2024.

[94] Enneng Yang, Li Shen, Guibing Guo, Xingwei Wang, Xiaochun Cao, Jie Zhang, and Dacheng Tao. Model merging in llms, mllms, and beyond: Methods, theories, applications and opportunities. *arXiv preprint arXiv:2408.07666*, 2024.

[95] Enneng Yang, Li Shen, Zhenyi Wang, Guibing Guo, Xiaojun Chen, Xingwei Wang, and Dacheng Tao. Representation surgery for multi-task model merging. *Forty-first International Conference on Machine Learning*, 2024.

[96] Enneng Yang, Zhenyi Wang, Li Shen, Shiwei Liu, Guibing Guo, Xingwei Wang, and Dacheng Tao. Adamerging: Adaptive model merging for multi-task learning. *The Twelfth International Conference on Learning Representations*, 2024.

[97] Peng Ye, Chenyu Huang, Mingzhu Shen, Tao Chen, Yongqi Huang, Yuning Zhang, and Wanli Ouyang. Merging vision transformers from different tasks and domains. *arXiv preprint arXiv:2312.16240*, 2023.

[98] Xin Yi, Shunfan Zheng, Linlin Wang, Xiaoling Wang, and Liang He. A safety realignment framework via subspace-oriented model fusion for large language models. *Knowledge-Based Systems*, 306:112701, 2024.

[99] Jaehong Yoon, Eunho Yang, Jeongtae Lee, and Sung Ju Hwang. Lifelong learning with dynamically expandable networks. *arXiv preprint arXiv:1708.01547*, 2017.

[100] Le Yu, Bowen Yu, Haiyang Yu, Fei Huang, and Yongbin Li. Language models are super mario: Absorbing abilities from homologous models as a free lunch. In *Forty-first International Conference on Machine Learning*, 2024.

[101] David Yunis, Kumar Kshitij Patel, Pedro Henrique Pamplona Savarese, Gal Vardi, Jonathan Frankle, Matthew Walter, Karen Livescu, and Michael Maire. On convexity and linear mode connectivity in neural networks. In *OPT 2022: Optimization for Machine Learning (NeurIPS 2022 Workshop)*, 2022.

[102] Friedemann Zenke, Ben Poole, and Surya Ganguli. Continual learning through synaptic intelligence. In *International conference on machine learning*, pages 3987–3995. PMLR, 2017.

[103] Chujie Zheng, Ziqi Wang, Heng Ji, Minlie Huang, and Nanyun Peng. Weak-to-strong extrapolation expedites alignment. In *ICML 2024 Workshop on Models of Human Feedback for AI Alignment*, 2024. URL `https://openreview.net/forum?id=DbyqbL4ztr`.

[104] Hongling Zheng, Li Shen, Anke Tang, Yong Luo, Han Hu, Bo Du, and Dacheng Tao. Learn from model beyond fine-tuning: A survey. *arXiv preprint arXiv:2310.08184*, 2023.

[105] Da-Wei Zhou, Hai-Long Sun, Jingyi Ning, Han-Jia Ye, and De-Chuan Zhan. Continual learning with pre-trained models: A survey. *arXiv preprint arXiv:2401.16386*, 2024.

[106] Yuyan Zhou, Liang Song, Bingning Wang, and Weipeng Chen. Metagpt: Merging large language models using model exclusive task arithmetic. *arXiv preprint arXiv:2406.11385*, 2024.

[107] Max Zimmer, Christoph Spiegel, and Sebastian Pokutta. Sparse model soups: A recipe for improved pruning via model averaging. *arXiv preprint arXiv:2306.16788*, 2023.

NeurIPS Paper Checklist

1. **Claims**

   Question: Do the main claims made in the abstract and introduction accurately reflect the paper's contributions and scope?

   Answer: [Yes]

   Justification: The abstract and introduction clearly state that we propose Orthogonal Projection-based Continual Merging (OPCM), a sequential approach to merging multiple fine-tuned models that enables constant memory complexity. These claims are accurately reflected throughout the paper with theoretical analysis and empirical evaluation.

   Guidelines:

   - The answer NA means that the abstract and introduction do not include the claims made in the paper.
   - The abstract and/or introduction should clearly state the claims made, including the contributions made in the paper and important assumptions and limitations. A No or NA answer to this question will not be perceived well by the reviewers.
   - The claims made should match theoretical and experimental results, and reflect how much the results can be expected to generalize to other settings.
   - It is fine to include aspirational goals as motivation as long as it is clear that these goals are not attained by the paper.

2. **Limitations**

   Question: Does the paper discuss the limitations of the work performed by the authors?

   Answer: [Yes]

   Justification: The paper discusses limitations in Section 3.2 regarding the non-commutative nature of continual merging and how task ordering affects final performance. Additional computational complexity considerations of the SVD-based orthogonal projection are discussed in Appendix B.

   Guidelines:

   - The answer NA means that the paper has no limitation while the answer No means that the paper has limitations, but those are not discussed in the paper.
   - The authors are encouraged to create a separate "Limitations" section in their paper.
   - The paper should point out any strong assumptions and how robust the results are to violations of these assumptions (e.g., independence assumptions, noiseless settings, model well-specification, asymptotic approximations only holding locally). The authors should reflect on how these assumptions might be violated in practice and what the implications would be.
   - The authors should reflect on the scope of the claims made, e.g., if the approach was only tested on a few datasets or with a few runs. In general, empirical results often depend on implicit assumptions, which should be articulated.
   - The authors should reflect on the factors that influence the performance of the approach. For example, a facial recognition algorithm may perform poorly when image resolution is low or images are taken in low lighting. Or a speech-to-text system might not be used reliably to provide closed captions for online lectures because it fails to handle technical jargon.
   - The authors should discuss the computational efficiency of the proposed algorithms and how they scale with dataset size.
   - If applicable, the authors should discuss possible limitations of their approach to address problems of privacy and fairness.
   - While the authors might fear that complete honesty about limitations might be used by reviewers as grounds for rejection, a worse outcome might be that reviewers discover limitations that aren't acknowledged in the paper. The authors should use their best judgment and recognize that individual actions in favor of transparency play an important role in developing norms that preserve the integrity of the community. Reviewers will be specifically instructed to not penalize honesty concerning limitations.

3. **Theory assumptions and proofs**

   Question: For each theoretical result, does the paper provide the full set of assumptions and a complete (and correct) proof?

   Answer:[Yes]

   Justification: All theoretical results presented in Section 5 (including Theorem 5.1, Theorem 5.2, and Corollary 5.3) are accompanied by detailed proofs in Appendix A.1.

   Guidelines:

   - The answer NA means that the paper does not include theoretical results.
   - All the theorems, formulas, and proofs in the paper should be numbered and cross-referenced.
   - All assumptions should be clearly stated or referenced in the statement of any theorems.
   - The proofs can either appear in the main paper or the supplemental material, but if they appear in the supplemental material, the authors are encouraged to provide a short proof sketch to provide intuition.
   - Inversely, any informal proof provided in the core of the paper should be complemented by formal proofs provided in appendix or supplemental material.
   - Theorems and Lemmas that the proof relies upon should be properly referenced.

4. **Experimental result reproducibility**

   Question: Does the paper fully disclose all the information needed to reproduce the main experimental results of the paper to the extent that it affects the main claims and/or conclusions of the paper (regardless of whether the code and data are provided or not)?

   Answer: [Yes]

   Justification: The paper provides detailed information about the experimental setup, including dataset details, model architectures, and hyperparameters in Section 6 and Appendix D. The implementation details of the continual merging algorithm are clearly described in Algorithm 1 and code is publically available via anonymous repository.

   Guidelines:

   - The answer NA means that the paper does not include experiments.
   - If the paper includes experiments, a No answer to this question will not be perceived well by the reviewers: Making the paper reproducible is important, regardless of whether the code and data are provided or not.
   - If the contribution is a dataset and/or model, the authors should describe the steps taken to make their results reproducible or verifiable.
   - Depending on the contribution, reproducibility can be accomplished in various ways. For example, if the contribution is a novel architecture, describing the architecture fully might suffice, or if the contribution is a specific model and empirical evaluation, it may be necessary to either make it possible for others to replicate the model with the same dataset, or provide access to the model. In general. releasing code and data is often one good way to accomplish this, but reproducibility can also be provided via detailed instructions for how to replicate the results, access to a hosted model (e.g., in the case of a large language model), releasing of a model checkpoint, or other means that are appropriate to the research performed.
   - While NeurIPS does not require releasing code, the conference does require all submissions to provide some reasonable avenue for reproducibility, which may depend on the nature of the contribution. For example
     (a) If the contribution is primarily a new algorithm, the paper should make it clear how to reproduce that algorithm.
     (b) If the contribution is primarily a new model architecture, the paper should describe the architecture clearly and fully.
     (c) If the contribution is a new model (e.g., a large language model), then there should either be a way to access this model for reproducing the results or a way to reproduce the model (e.g., with an open-source dataset or instructions for how to construct the dataset).

(d) We recognize that reproducibility may be tricky in some cases, in which case authors are welcome to describe the particular way they provide for reproducibility. In the case of closed-source models, it may be that access to the model is limited in some way (e.g., to registered users), but it should be possible for other researchers to have some path to reproducing or verifying the results.

5. **Open access to data and code**

   Question: Does the paper provide open access to the data and code, with sufficient instructions to faithfully reproduce the main experimental results, as described in supplemental material?

   Answer: [Yes]

   Justification: The datasets used in the experiments are publicly available, and the code is publically available via anonymous repository.

   Guidelines:

   - The answer NA means that paper does not include experiments requiring code.
   - Please see the NeurIPS code and data submission guidelines (`https://nips.cc/public/guides/CodeSubmissionPolicy`) for more details.
   - While we encourage the release of code and data, we understand that this might not be possible, so "No" is an acceptable answer. Papers cannot be rejected simply for not including code, unless this is central to the contribution (e.g., for a new open-source benchmark).
   - The instructions should contain the exact command and environment needed to run to reproduce the results. See the NeurIPS code and data submission guidelines (`https://nips.cc/public/guides/CodeSubmissionPolicy`) for more details.
   - The authors should provide instructions on data access and preparation, including how to access the raw data, preprocessed data, intermediate data, and generated data, etc.
   - The authors should provide scripts to reproduce all experimental results for the new proposed method and baselines. If only a subset of experiments are reproducible, they should state which ones are omitted from the script and why.
   - At submission time, to preserve anonymity, the authors should release anonymized versions (if applicable).
   - Providing as much information as possible in supplemental material (appended to the paper) is recommended, but including URLs to data and code is permitted.

6. **Experimental setting/details**

   Question: Does the paper specify all the training and test details (e.g., data splits, hyperparameters, how they were chosen, type of optimizer, etc.) necessary to understand the results?

   Answer: [Yes]

   Justification: The paper provides detailed information about the experimental setup, including dataset details, model architectures, and hyperparameters in Section 6 and Appendix D.

   Guidelines:

   - The answer NA means that the paper does not include experiments.
   - The experimental setting should be presented in the core of the paper to a level of detail that is necessary to appreciate the results and make sense of them.
   - The full details can be provided either with the code, in appendix, or as supplemental material.

7. **Experiment statistical significance**

   Question: Does the paper report error bars suitably and correctly defined or other appropriate information about the statistical significance of the experiments?

   Answer: [Yes]

   Justification: Our tables and figures include standard deviations across multiple runs with different task orderings, clearly showing the robustness of our method compared to baselines.

   Guidelines:

- The answer NA means that the paper does not include experiments.
- The authors should answer "Yes" if the results are accompanied by error bars, confidence intervals, or statistical significance tests, at least for the experiments that support the main claims of the paper.
- The factors of variability that the error bars are capturing should be clearly stated (for example, train/test split, initialization, random drawing of some parameter, or overall run with given experimental conditions).
- The method for calculating the error bars should be explained (closed form formula, call to a library function, bootstrap, etc.)
- The assumptions made should be given (e.g., Normally distributed errors).
- It should be clear whether the error bar is the standard deviation or the standard error of the mean.
- It is OK to report 1-sigma error bars, but one should state it. The authors should preferably report a 2-sigma error bar than state that they have a 96% CI, if the hypothesis of Normality of errors is not verified.
- For asymmetric distributions, the authors should be careful not to show in tables or figures symmetric error bars that would yield results that are out of range (e.g. negative error rates).
- If error bars are reported in tables or plots, The authors should explain in the text how they were calculated and reference the corresponding figures or tables in the text.

8. **Experiments compute resources**

   Question: For each experiment, does the paper provide sufficient information on the computer resources (type of compute workers, memory, time of execution) needed to reproduce the experiments?

   Answer: [Yes]

   Justification: Appendix D.1 provides details on the computational resources used, including GPU types, memory requirements.

   Guidelines:

   - The answer NA means that the paper does not include experiments.
   - The paper should indicate the type of compute workers CPU or GPU, internal cluster, or cloud provider, including relevant memory and storage.
   - The paper should provide the amount of compute required for each of the individual experimental runs as well as estimate the total compute.
   - The paper should disclose whether the full research project required more compute than the experiments reported in the paper (e.g., preliminary or failed experiments that didn't make it into the paper).

9. **Code of ethics**

   Question: Does the research conducted in the paper conform, in every respect, with the NeurIPS Code of Ethics `https://neurips.cc/public/EthicsGuidelines`?

   Answer: [Yes]

   Justification: Our research adheres to the NeurIPS Code of Ethics.

   Guidelines:

   - The answer NA means that the authors have not reviewed the NeurIPS Code of Ethics.
   - If the authors answer No, they should explain the special circumstances that require a deviation from the Code of Ethics.
   - The authors should make sure to preserve anonymity (e.g., if there is a special consideration due to laws or regulations in their jurisdiction).

10. **Broader impacts**

    Question: Does the paper discuss both potential positive societal impacts and negative societal impacts of the work performed?

    Answer: [Yes]

Justification: Section 7 discusses the potential positive impacts (enabling more efficient model deployment, reducing computational resources).

Guidelines:

- The answer NA means that there is no societal impact of the work performed.
- If the authors answer NA or No, they should explain why their work has no societal impact or why the paper does not address societal impact.
- Examples of negative societal impacts include potential malicious or unintended uses (e.g., disinformation, generating fake profiles, surveillance), fairness considerations (e.g., deployment of technologies that could make decisions that unfairly impact specific groups), privacy considerations, and security considerations.
- The conference expects that many papers will be foundational research and not tied to particular applications, let alone deployments. However, if there is a direct path to any negative applications, the authors should point it out. For example, it is legitimate to point out that an improvement in the quality of generative models could be used to generate deepfakes for disinformation. On the other hand, it is not needed to point out that a generic algorithm for optimizing neural networks could enable people to train models that generate Deepfakes faster.
- The authors should consider possible harms that could arise when the technology is being used as intended and functioning correctly, harms that could arise when the technology is being used as intended but gives incorrect results, and harms following from (intentional or unintentional) misuse of the technology.
- If there are negative societal impacts, the authors could also discuss possible mitigation strategies (e.g., gated release of models, providing defenses in addition to attacks, mechanisms for monitoring misuse, mechanisms to monitor how a system learns from feedback over time, improving the efficiency and accessibility of ML).

11. **Safeguards**

Question: Does the paper describe safeguards that have been put in place for responsible release of data or models that have a high risk for misuse (e.g., pretrained language models, image generators, or scraped datasets)?

Answer: [NA]

Justification: Our paper presents a methodology for merging existing models rather than releasing new models or datasets with high risk for misuse.

Guidelines:

- The answer NA means that the paper poses no such risks.
- Released models that have a high risk for misuse or dual-use should be released with necessary safeguards to allow for controlled use of the model, for example by requiring that users adhere to usage guidelines or restrictions to access the model or implementing safety filters.
- Datasets that have been scraped from the Internet could pose safety risks. The authors should describe how they avoided releasing unsafe images.
- We recognize that providing effective safeguards is challenging, and many papers do not require this, but we encourage authors to take this into account and make a best faith effort.

12. **Licenses for existing assets**

Question: Are the creators or original owners of assets (e.g., code, data, models), used in the paper, properly credited and are the license and terms of use explicitly mentioned and properly respected?

Answer: [Yes]

Justification: We properly cite and credit the CLIP models and all datasets used in our experiments, with appropriate references to the original papers and licenses.

Guidelines:

- The answer NA means that the paper does not use existing assets.
- The authors should cite the original paper that produced the code package or dataset.

- The authors should state which version of the asset is used and, if possible, include a URL.
- The name of the license (e.g., CC-BY 4.0) should be included for each asset.
- For scraped data from a particular source (e.g., website), the copyright and terms of service of that source should be provided.
- If assets are released, the license, copyright information, and terms of use in the package should be provided. For popular datasets, `paperswithcode.com/datasets` has curated licenses for some datasets. Their licensing guide can help determine the license of a dataset.
- For existing datasets that are re-packaged, both the original license and the license of the derived asset (if it has changed) should be provided.
- If this information is not available online, the authors are encouraged to reach out to the asset's creators.

13. **New assets**

    Question: Are new assets introduced in the paper well documented and is the documentation provided alongside the assets?

    Answer: [Yes]

    Justification: Our code implementation of OPCM is documented with detailed comments, usage examples.

    Guidelines:

    - The answer NA means that the paper does not release new assets.
    - Researchers should communicate the details of the dataset/code/model as part of their submissions via structured templates. This includes details about training, license, limitations, etc.
    - The paper should discuss whether and how consent was obtained from people whose asset is used.
    - At submission time, remember to anonymize your assets (if applicable). You can either create an anonymized URL or include an anonymized zip file.

14. **Crowdsourcing and research with human subjects**

    Question: For crowdsourcing experiments and research with human subjects, does the paper include the full text of instructions given to participants and screenshots, if applicable, as well as details about compensation (if any)?

    Answer: [NA]

    Justification: Our research does not involve crowdsourcing or human subjects.

    Guidelines:

    - The answer NA means that the paper does not involve crowdsourcing nor research with human subjects.
    - Including this information in the supplemental material is fine, but if the main contribution of the paper involves human subjects, then as much detail as possible should be included in the main paper.
    - According to the NeurIPS Code of Ethics, workers involved in data collection, curation, or other labor should be paid at least the minimum wage in the country of the data collector.

15. **Institutional review board (IRB) approvals or equivalent for research with human subjects**

    Question: Does the paper describe potential risks incurred by study participants, whether such risks were disclosed to the subjects, and whether Institutional Review Board (IRB) approvals (or an equivalent approval/review based on the requirements of your country or institution) were obtained?

    Answer: [NA]

    Justification: Our research does not involve human subjects, so IRB approval was not required.

Guidelines:

- The answer NA means that the paper does not involve crowdsourcing nor research with human subjects.
- Depending on the country in which research is conducted, IRB approval (or equivalent) may be required for any human subjects research. If you obtained IRB approval, you should clearly state this in the paper.
- We recognize that the procedures for this may vary significantly between institutions and locations, and we expect authors to adhere to the NeurIPS Code of Ethics and the guidelines for their institution.
- For initial submissions, do not include any information that would break anonymity (if applicable), such as the institution conducting the review.

16. **Declaration of LLM usage**

    Question: Does the paper describe the usage of LLMs if it is an important, original, or non-standard component of the core methods in this research? Note that if the LLM is used only for writing, editing, or formatting purposes and does not impact the core methodology, scientific rigorousness, or originality of the research, declaration is not required.

    Answer: [NA]

    Justification: Our research does not use LLMs as a component of our core methodology.

    Guidelines:

    - The answer NA means that the core method development in this research does not involve LLMs as any important, original, or non-standard components.
    - Please refer to our LLM policy (`https://neurips.cc/Conferences/2025/LLM`) for what should or should not be described.

The appendix is organized into several sections, each providing additional insights and details related to different aspects of the main work.

The appendix is divided into several sections, each giving extra information and details.

A Additional Theoretical Analysis

A.1 Proofs of Theorems

In this section, we provide detailed proofs for the theorems and corollaries presented in the main text.

First, we prove the general term formula of the merged model, which demonstrates that the merged model can be expressed as a weighted combination of all previous task-specific models. This formula shows how each task's contribution is preserved through its projection operator and serves as the foundation for understanding the key properties of our continual merging approach.

Theorem A.1 (General Term Formula)**.** *Given the update rule of our method as defined in Eq.(6), the general term formula of the merged model at time step t can be expressed as:*

$$W_{merged}^{(t)} = W^{(0)} + \frac{1}{\lambda^{(t)}} \sum_{i=1}^{t} \mathcal{P}_{\alpha}^{(i-1)} \left(\Delta W^{(i)} \right). \tag{12}$$

Proof. We prove the general term formula by mathematical induction. For the base case $t = 1$, we have $W_{\text{merged}}^{(1)} = W^{(1)} = W^{(0)} + \frac{\mathcal{P}_{\alpha}^{(0)}(\Delta W^{(1)})}{\lambda^{(1)}}$, where $\mathcal{P}_{\alpha}^{(0)}$ is the identity mapping and $\lambda^{(1)} = 1$. For $t = 2$, applying the update rule yields:

$$W_{\text{merged}}^{(2)} = W^{(0)} + \frac{\lambda^{(1)} \Delta W_{\text{merged}}^{(1)} + \mathcal{P}_{\alpha}^{(1)} \left(\Delta W^{(2)} \right)}{\lambda^{(2)}}, \tag{13}$$

$$= W^{(0)} + \frac{\lambda^{(1)} \frac{\mathcal{P}_{\alpha}^{(0)}\left(\Delta W^{(1)}\right)}{\lambda^{(1)}} + \mathcal{P}_{\alpha}^{(1)} \left(\Delta W^{(2)} \right)}{\lambda^{(2)}}, \tag{14}$$

$$= W^{(0)} + \underbrace{\frac{\mathcal{P}_{\alpha}^{(0)} \left(\Delta W^{(1)} \right) + \mathcal{P}_{\alpha}^{(1)} \left(\Delta W^{(2)} \right)}{\lambda^{(2)}}}_{\Delta W_{\text{merged}}^{(2)}}. \tag{15}$$

Thus, the formula holds for $t \leq 2$. For the inductive step, assume the formula holds for $t = k-1$. Then for $t = k$:

$$W_{\text{merged}}^{(k)} = W^{(0)} + \frac{\lambda^{(k-1)} \Delta W_{\text{merged}}^{(k-1)} + \mathcal{P}_\alpha^{(k-1)}\left(\Delta W^{(k)}\right)}{\lambda^{(k)}}, \tag{16}$$

$$= W^{(0)} + \frac{\lambda^{(k-1)} \left(\frac{1}{\lambda^{(k-1)}} \sum_{i=1}^{k-1} \mathcal{P}_\alpha^{(i-1)}\left(\Delta W^{(i)}\right)\right) + \mathcal{P}_\alpha^{(k-1)}\left(\Delta W^{(k)}\right)}{\lambda^{(k)}}, \tag{17}$$

$$= W^{(0)} + \frac{1}{\lambda^{(k)}} \sum_{i=1}^{k} \mathcal{P}_\alpha^{(i-1)}\left(\Delta W^{(i)}\right). \tag{18}$$

By the principle of mathematical induction, the formula holds for all $t \geq 1$. □

A fundamental property of our method is the orthogonality between the projected task vectors and the previously merged model. This orthogonality property is essential as it guarantees that new task vectors do not interfere with previously acquired knowledge, thereby preventing catastrophic forgetting.

Proof of Theorem 5.1. By definition of the projection mapping $\mathcal{P}_\alpha^{(t-1)}$, we have:

$$\left\langle \mathcal{P}_\alpha^{(t-1)}(\Delta W^{(t)}), \Delta W_{\text{merged}}^{(t-1)} \right\rangle_F = \left\langle \sum_{i,j=r_\alpha, i\neq j}^{m,n} \left\langle \Delta W^{(t)}, u_i v_j^T \right\rangle_F u_i v_j^T, U^{(t-1)} \Sigma^{(t-1)} V^{(t-1)T} \right\rangle_F, \tag{19}$$

$$= \sum_{i,j=r_\alpha, i\neq j}^{m,n} \left\langle \Delta W^{(t)}, u_i v_j^T \right\rangle_F \left\langle u_i v_j^T, U^{(t-1)} \Sigma^{(t-1)} V^{(t-1)T} \right\rangle_F. \tag{20}$$

Since $U^{(t-1)} \Sigma^{(t-1)} V^{(t-1)T}$ represents the SVD of $\Delta W_{\text{merged}}^{(t-1)}$, where the columns of $U^{(t-1)}$ and $V^{(t-1)}$ form orthonormal bases, for any pair (i, j) where $i \neq j$, we have $\left\langle u_i v_j^T, U^{(t-1)} \Sigma^{(t-1)} V^{(t-1)T} \right\rangle_F = 0$ due to the orthogonality of singular vectors. Therefore:

$$\left\langle \mathcal{P}_\alpha^{(t-1)}(\Delta W^{(t)}), \Delta W_{\text{merged}}^{(t-1)} \right\rangle_F = 0. \tag{21}$$

□

Finally, we prove the bounded distance theorem, which establishes that the distance between the merged model and the base model is bounded by the maximum distance between any task-specific model and the base model. This property provides a theoretical guarantee that the merged model remains within a controlled region around the base model, preventing catastrophic drift while allowing for effective adaptation to new tasks.

Proof of Theorem 5.2. We proceed by induction on t. For the base case $t = 1$, we have $W_{\text{merged}}^{(1)} - W^{(0)} = \Delta W^{(1)}$, so the bound holds trivially.

Assume the bound holds for $t-1$. For step t, using Eq.(6) and the orthogonality property of the projection operator:

$$\left\| W_{\text{merged}}^{(t)} - W^{(0)} \right\|_F^2 = \left\| \frac{\sqrt{t-1} \Delta W_{\text{merged}}^{(t-1)} + \mathcal{P}_\alpha^{(t-1)}(\Delta W^{(t)})}{\sqrt{t}} \right\|_F^2, \tag{22}$$

$$= \frac{t-1}{t} \left\| \Delta W_{\text{merged}}^{(t-1)} \right\|_F^2 + \frac{1}{t} \left\| \mathcal{P}_\alpha^{(t-1)}(\Delta W^{(t)}) \right\|_F^2. \tag{23}$$

By the properties of the projection operator, we know that $\left\|\mathcal{P}_{\alpha}^{(t-1)}\left(\Delta W^{(t)}\right)\right\|_F^2 \leq \left\|\Delta W^{(t)}\right\|_F^2$. Applying the induction hypothesis:

$$\left\|W_{\text{merged}}^{(t)} - W^{(0)}\right\|_F^2 \leq \frac{t-1}{t} \max_{i\in[1,t-1]} \left\|\Delta W^{(i)}\right\|_F^2 + \frac{1}{t}\left\|\Delta W^{(t)}\right\|_F^2, \tag{24}$$

$$\leq \max_{i\in[1,t]} \left\|\Delta W^{(i)}\right\|_F^2. \tag{25}$$

This completes the induction, proving the bound holds for all $t \geq 1$. □

A.2 Theoretical Analysis of Correlated Task Vectors

Another important theoretical consideration in continual model merging is how the projection mechanism handles correlated task vectors, where two task-specific models are highly similar to each other. We analyze this scenario to demonstrate another advantageous property of our approach.

Corollary A.2 (Efficient Handling of Correlated Task Vectors)**.** *Consider two task vectors $\Delta W^{(t-1)}$ and $\Delta W^{(t)}$ with high correlation. After incorporating $\Delta W^{(t-1)}$ into $W_{merged}^{(t-1)}$, the contribution of $\Delta W^{(t)}$ to the merged model is automatically filtered to include only novel information not present in $W_{merged}^{(t-1)}$.*

Proof. Due to the high correlation between task vectors, we can decompose $\Delta W^{(t)}$ as follows:

$$\Delta W^{(t)} = \rho \Delta W_{\text{merged}}^{(t-1)} + \eta, \tag{26}$$

where ρ is a scalar representing the correlation coefficient (high when vectors are strongly correlated) and η is a component orthogonal to $\Delta W_{\text{merged}}^{(t-1)}$, i.e., $\langle \eta, \Delta W_{\text{merged}}^{(t-1)} \rangle_F = 0$. Applying our projection operator, we have:

$$\mathcal{P}_{\alpha}^{(t-1)}(\Delta W^{(t)}) = \mathcal{P}_{\alpha}^{(t-1)}(\rho \Delta W_{\text{merged}}^{(t-1)} + \eta) \tag{27}$$

$$= \rho \mathcal{P}_{\alpha}^{(t-1)}(\Delta W_{\text{merged}}^{(t-1)}) + \mathcal{P}_{\alpha}^{(t-1)}(\eta) \tag{28}$$

By Theorem 5.1, $\mathcal{P}_{\alpha}^{(t-1)}(\Delta W_{\text{merged}}^{(t-1)}) = 0$ since $\Delta W_{\text{merged}}^{(t-1)}$ is orthogonal to its own projection. Additionally, since η is already orthogonal to $\Delta W_{\text{merged}}^{(t-1)}$, we have $\mathcal{P}_{\alpha}^{(t-1)}(\eta) = \eta$. Therefore:

$$\mathcal{P}_{\alpha}^{(t-1)}(\Delta W^{(t)}) = \eta \tag{29}$$

Consequently, the update for the merged model becomes:

$$W_{\text{merged}}^{(t)} = W^{(0)} + \frac{\lambda^{(t-1)} \Delta W_{\text{merged}}^{(t-1)} + \eta}{\lambda^{(t)}} \tag{30}$$

When the correlation is high, $|\eta|$ will be small, resulting in a minimal parameter update from the second task, which is precisely what we want for highly correlated task vectors. This demonstrates that the orthogonal projection mechanism of our method:

1. Automatically filters redundant knowledge in $\Delta W^{(t)}$ that is already captured in $W_{\text{merged}}^{(t-1)}$.
2. Incorporates only the novel information (η) into the merged model.
3. Prevents over-representation of similar concepts across multiple tasks, which could lead to catastrophic forgetting or overfitting to specific patterns.

□

This result has important practical implications. In scenarios where new task models are highly similar to previously merged models, our projection approach automatically adjusts the magnitude of parameter updates based on the novelty of the information. This automatic filtering mechanism contributes to the stability and effectiveness of the continual merging process, particularly when dealing with a sequence of related tasks.

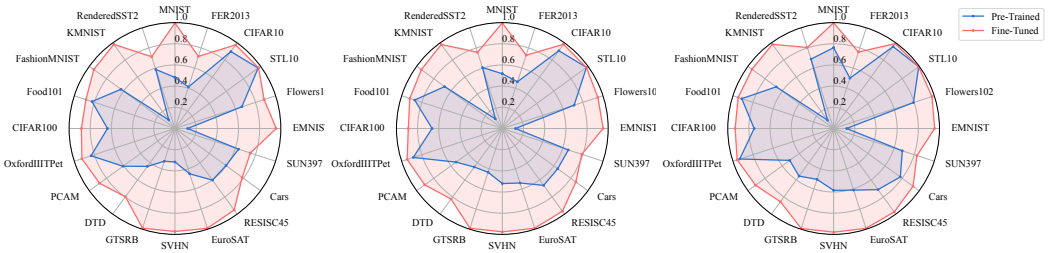

(a) ViT-B/32 (b) ViT-B/16 (c) ViT-L/14

Figure 8: Comparison of test set accuracy between the pre-trained model and individual fine-tuned models on different downstream tasks.

B Computational Complexity

We briefly discussed the memory complexity in Section 3.2, showing $O(|\theta|)$ constant memory complexity for continual model merging versus $O(T|\theta|)$ for conventional merging approaches. Here we discuss the computational complexity of OPCM. The computational complexity of OPCM is primarily dominated by the SVD decomposition, for each weight matrix $W \in \mathbb{R}^{m\times n}$, computing the full SVD has complexity $O(\min(m^2n, n^2m))$. Therefore, for T tasks and L linear layers, the complexity is approximately $O(TL\min(mn, mn))$.

Table 2: This table shows the runtime of different methods.

Method	Wall-Clock Time of Merging	Wall-Clock Time per Model
Continual Task Arithmetic	0.37s	≈0.04s
Continual Ties Merging	15.65s	≈2s
AdaMerging (Conventional Model Merging)	10.47min	≈78.5s
AdaMerging (Continual Model Merging)	11.85min	≈88.9s
OPCM	73.26s	≈9.1s

In Table 2, we show the runtime of different methods, including AdaMerging [96], Continual Task Arithmetic [29], Continual Ties Merging [91], and OPCM (the details of the compared baseline methods can be found in Appendices D.3.1 and E). As shown in the Table, our method is much faster than test-time adaptation-based methods like AdaMerging, while maintaining runtime in the same order of magnitude as training-free methods like Task Arithmetic and Ties-Merging.

C Details of the Fine-Tuned Models

In this section, we present the experimental details of model fine-tuning and evaluate the performance of the pre-trained model (zero-shot test accuracy) and our fine-tuned models on the test set of each downstream task. For each downstream task, we fine-tuned the visual encoder of the pre-trained CLIP-ViT models using task-specific training data, the classification heads are initialized using the pre-trained text encoder and fixed throughout the fine-tuning process. We employed a standard fine-tuning protocol with cross-entropy loss and the Adam optimizer, using a cosine annealing learning rate schedule with a maximum learning rate of 1e-5 and batch size 128, and train for 4000 steps [2].

Models and datasets. We adopt the same experimental setup as described in [83], where we fine-tune three different sizes of CLIP-ViT models (ViT-B/32, ViT-B/16, and ViT-L/14) on 20 downstream image classification tasks. All the models and datasets are publicly available on Hugging Face [85]. The 20 downstream tasks are SUN397 [88], Cars [39], RESISC45 [10], EuroSAT [26], SVHN [55], GTSRB [71], MNIST [41], DTD [11], Flowers102 [57], PCAM [80], FER2013 [24], OxfordIIITPet [60], STL10 [13], CIFAR100, CIFAR10 [40], Food101 [4], FashionMNIST [87], EMNIST [14], KMNIST [12], and RenderedSST2 [70, 63].

[2]The models are fine-tuned and evaluated using the FusionBench [75].

Table 3: Test set accuracy of the pre-trained model and individual fine-tuned models on different downstream tasks.

Model	SUN397	Cars	RESISC45	EuroSAT	SVHN	GTSRB	MNIST	DTD	Flowers102	PCAM
					CLIP-ViT-B/32					
Pre-trained	63.2	59.6	60.3	45.0	31.6	32.5	48.3	44.2	66.4	60.6
Fine-tuned	74.9	78.5	95.1	99.1	97.3	98.9	99.6	79.7	88.6	88.0
					CLIP-ViT-B/16					
Pre-trained	65.5	64.7	66.4	54.1	52.0	43.5	51.7	45.0	71.3	54.0
Fine-tuned	78.9	85.9	96.6	99.0	97.6	99.0	99.7	82.3	94.9	90.6
					CLIP-ViT-L/14					
Pre-trained	68.2	77.9	71.3	61.2	58.4	50.5	76.3	55.5	79.2	51.2
Fine-tuned	82.8	92.8	97.4	99.1	97.9	99.2	99.8	85.5	97.7	91.1

Model	FER2013	OxfordIIITPet	STL10	CIFAR100	CIFAR10	Food101	FashionMNIST	EMNIST	KMNIST	RenderedSST2
					CLIP-ViT-B/32					
Pre-trained	41.3	83.3	97.1	63.7	89.8	82.4	63.0	12.0	10.0	58.6
Fine-tuned	71.6	92.5	97.5	88.4	97.6	88.4	94.7	95.6	98.2	71.3
					CLIP-ViT-B/16					
Pre-trained	46.4	88.4	98.3	66.3	90.8	87.0	67.3	12.4	11.2	60.6
Fine-tuned	72.8	94.5	98.2	88.8	98.3	91.9	94.5	95.3	98.1	75.7
					CLIP-ViT-L/14					
Pre-trained	50.0	93.2	99.4	75.1	95.6	91.2	67.0	12.3	9.7	68.9
Fine-tuned	75.9	95.7	99.2	93.0	99.1	94.8	95.3	95.4	98.3	80.5

In the fine-tuning process, only the vision encoder was adjusted, while the text encoder remained unchanged. The pre-trained text encoder was used to generate (zero-shot)task-specific classification heads, and the classification heads were also fixed throughout the fine-tuning process. This means that both the pre-trained and fine-tuned models utilize the same classification heads for a given task. This approach preserves the open-vocabulary capability of the model, allowing it to remain applicable to any downstream task. Additionally, freezing the classification head does not compromise accuracy as shown in [28].

Figure 8 and Table 3 demonstrate the performance comparison between pre-trained and fine-tuned models across 20 downstream tasks. As illustrated, fine-tuning consistently improves model performance across all architectures (ViT-B/16, ViT-B/32, and ViT-L/14), with particularly notable gains in task-specific accuracy for most tasks.

Figures 9, 10, and 11 present the cosine similarity matrices between task vectors for CLIP-ViT models of different sizes (B/32, B/16, and L/14) fine-tuned on 20 downstream tasks. Several key observations emerge from these visualizations: (1) Most off-diagonal elements show very low cosine similarity values (0.01-0.05), indicating that the majority of task vectors are largely orthogonal to each other. (2) The similarity patterns remain largely consistent across different model architectures, though ViT-L/14 shows slightly lower similarity values overall, suggesting that larger models may learn more specialized representations for each task. (3) Some groups of related tasks show slightly elevated similarity values, indicating that the tasks are more similar to each other. For example,

- Digit recognition tasks (SVHN,MNIST, EMNIST, KMNIST) exhibit higher mutual similarities.
- Natural image classification tasks (CIFAR10, CIFAR100) show moderate correlations.

In most of the experiments, we group the tasks into 8, 14, and 20 tasks, and report the average accuracy (ACC) and backward transfer (BWT) of the merged models. The task groups are as follows:

- The 8 tasks: SUN397, Cars, RESISC45, EuroSAT, SVHN, GTSRB, MNIST, and DTD
- The 14 tasks: the 8 tasks together with Flowers102, PCAM, FER2013, OxfordIIITPet, STL10, and CIFAR100.
- The 20 tasks: the 14 tasks together with CIFAR10, Food101, FashionMNIST, EMNIST, KMNIST, and RenderedSST2.

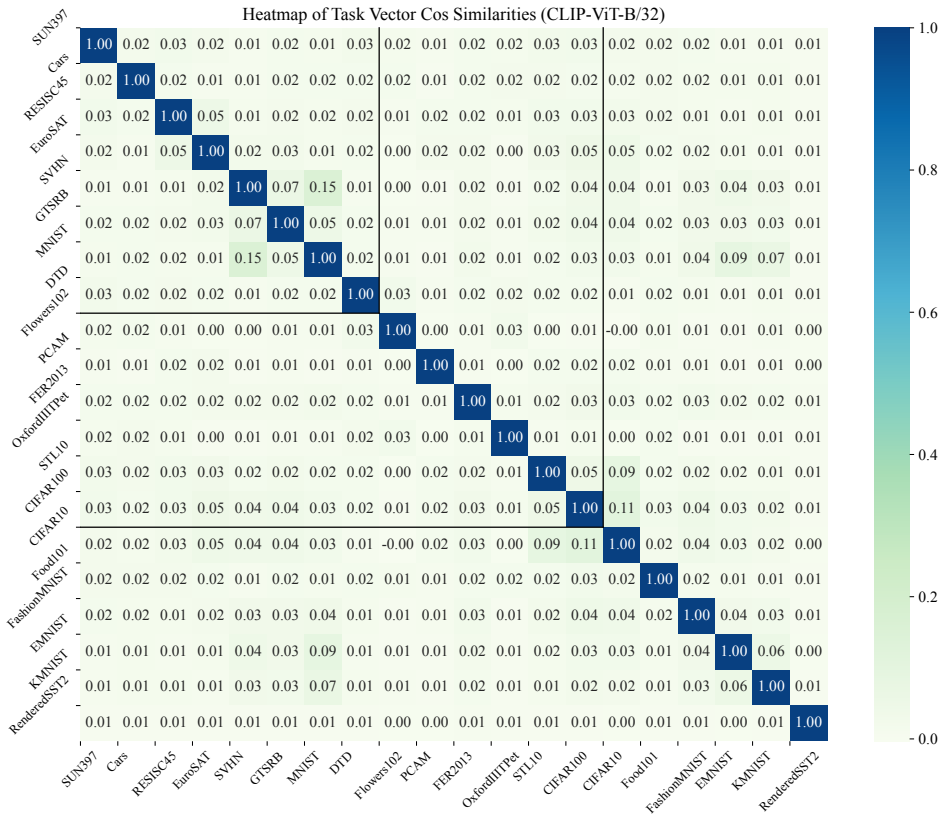

Figure 9: Cosine similarity between task vectors of CLIP-ViT-B/32 models fine-tuned on different downstream tasks.

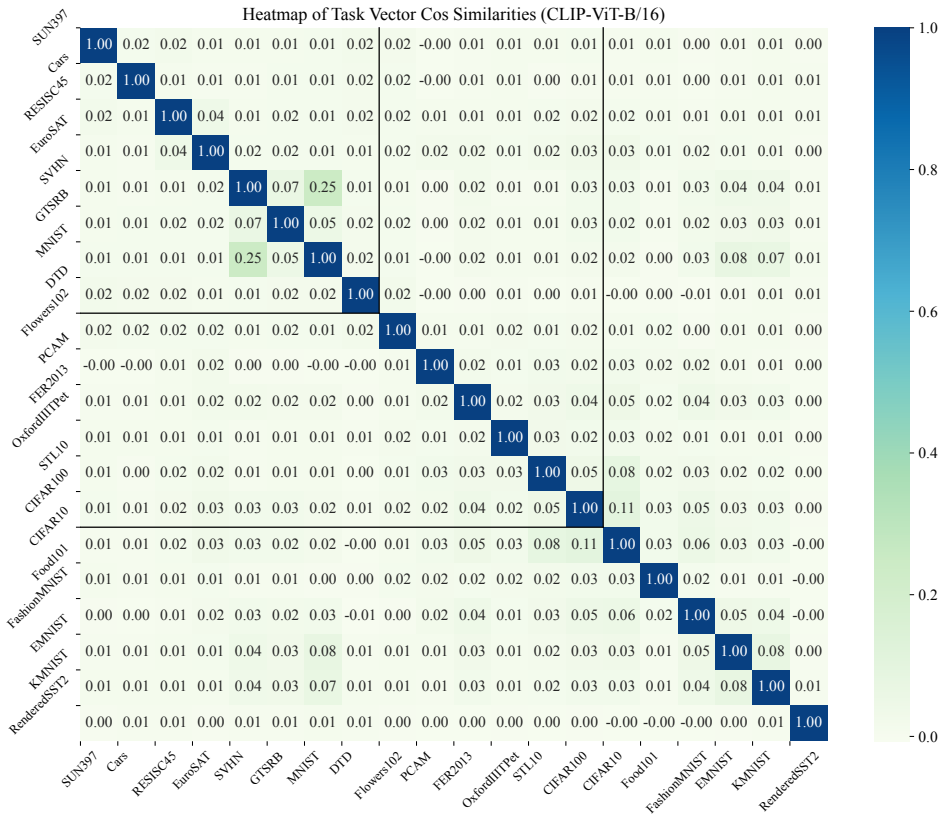

Figure 10: Cosine similarity between task vectors of CLIP-ViT-B/16 models fine-tuned on different downstream tasks.

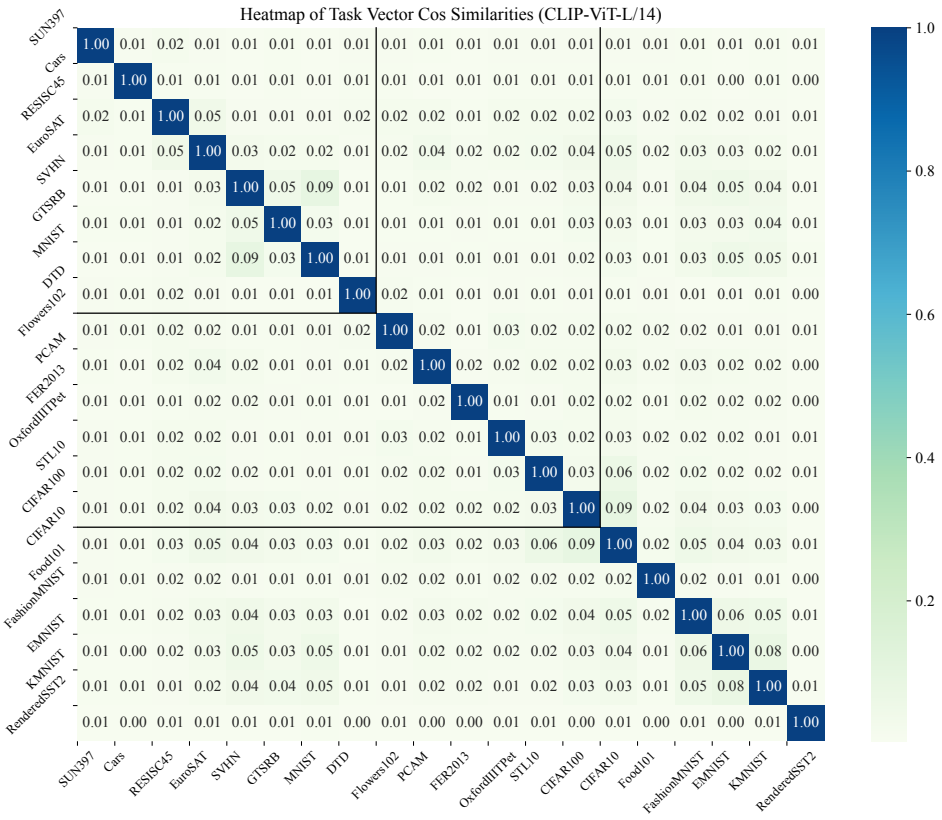

Figure 11: Cosine similarity between task vectors of CLIP-ViT-L/14 models fine-tuned on different downstream tasks.

D Additional Details on Experiments

D.1 Computational Resources

All experiments were conducted on a single machine with 8 NVIDIA RTX 4090 GPUs, each with 24GB of memory. The code was implemented in PyTorch and Python 3.12.

D.2 Evaluation Metrics

Here we provide the details of the evaluation metrics used in our experiments, including average accuracy (ACC) of the merged model at the final step and backward transfer (BWT).

$$\text{ACC}_{\text{avg}} = \frac{1}{T}\sum_{t=1}^{T}\text{ACC}_i\left(W_{\text{merged}}^{(T)}\right), \tag{31}$$

$$\text{BWT} = \frac{\sum_{i=1}^{T-1}\text{ACC}_i\left(\theta_{\text{merged}}^{(T)}\right) - \text{ACC}_i\left(\theta_{\text{merged}}^{(i)}\right)}{T-1}, \tag{32}$$

where $\theta_{\text{merged}}^{(i)}$ and $\theta_{\text{merged}}^{(T)}$ are the parameters of the merged model at i-th step and the final merged model, respectively. $\text{ACC}_i(\cdot)$ is the accuracy on the i-th task's test data.

D.3 Continual Multi-Task Model Merging

For our continual multi-task model merging experiments, we evaluated three different CLIP-ViT architectures (ViT-B/32, ViT-B/16, and ViT-L/14) on task sets of increasing size (8, 14, and 20 tasks). Each experiment was repeated 10 times with randomly shuffled task orders to ensure robust evaluation. The models were initialized using pre-trained CLIP checkpoints and subsequently fine-tuned separately for each task before being merged. During fine-tuning, only the vision encoder was updated, while the text encoder remained frozen and was employed to generate task-specific classification heads. For further details on the fine-tuning process, please see Appendix C.

D.3.1 Baseline Methods

In our experiments, we follow the common practice in model merging literature of using zero-shot classification heads initialized with the pre-trained CLIP model's text encoder. Specifically, we construct task-specific classification heads using CLIP's text encoder to generate zero-shot weights for each task's class names and templates. When fine-tuning the vision encoder, the classification head remains fixed. This is meant to preserve the open-vocabulary nature of the CLIP model, so it can still handle unseen classes during inference.

Continual Fine-tuning is a common baseline method for continual learning. For a sequence of tasks associate with training datasets $\{\mathcal{D}_1, \mathcal{D}_2, \ldots, \mathcal{D}_t\}$, the model is fine-tuned on each task sequentially. Denote the model parameters after fine-tuning on the i-th task as $\theta^{(i)}$. The update rule of continual fine-tuning is given by:

$$\theta^{(t)} = \text{Fine-tune}(\theta^{(t-1)}, \mathcal{D}_t), \tag{33}$$

where Fine-tune is the fine-tuning process. For each task, we use the same cosine annealing learning rate schedule with a maximum learning rate of 1e-5 and batch size 128, and train for 4000 steps. For continual fine-tuning, we set the random seed to 42 and shuffle the task order.

Stochastic weight averaging (SWA) is a common technique to stabilize the training process and improve generalization in model training [30]. The update rule of SWA is given by:

$$\theta_{\text{SWA}}^{(1)} = \theta^{(1)}, \quad \theta_{\text{SWA}}^{(t)} = \frac{\theta_{\text{SWA}}^{(t-1)}(t-1) + \theta^{(t)}}{t}, \tag{34}$$

where $\theta^{(t)}$ is the model parameters at step t, and $\theta_{\text{SWA}}^{(t)}$ is the averaged model parameters at step t. Expanding the above equation, we have:

$$\theta_{\text{SWA}}^{(t)} = \frac{1}{t}\sum_{i=1}^{t}\theta^{(i)}. \tag{35}$$

Therefore, this method is equivalent to averaging the parameters of all the checkpoints, which is also known as modelsoups in the literature [86, 107, 62].

Task Arithmetic is a simple yet powerful technique for merging multiple task-specific models into a unified multi-task model, as demonstrated in recent studies [29, 59]. This method linearly combines the parameters of task-specific fine-tuned models with those of the shared pre-trained base model, allowing the merged model to handle multiple tasks effectively at the same time. Mathematically, task arithmetic can be formalized as follows. Given a pre-trained model with parameters $\theta^{(0)}$ and a set of T task-specific models fine-tuned from the pre-trained model with parameters $\theta^{(i)}$ for $i = 1, 2, \ldots, T$, the parameters of the merged model θ_{merged} are computed as:

$$\theta_{\text{merged}} = \theta^{(0)} + \lambda \sum_{i=1}^{T} \left(\theta^{(i)} - \theta^{(0)} \right), \tag{36}$$

where λ is a scaling factor that is usually selected on a validation set using a grid search. In our experiments, we choose the value of λ that achieves the highest average accuracy from the set $\{0.1, 0.2, 0.3, 0.4, 0.5, 0.6, 0.7, 0.8, 0.9, 1.0\}$. The experimental results show that $\lambda = 0.3$ is the optimal value for eight image classification tasks, and $\lambda = 0.1$ is the optimal value for 14 and 20 tasks.

In our continual multi-task model merging experiments, we use the following update rule of the merged model at step t:

$$\theta^{(0)}_{\text{merged}} = \theta^{(0)}, \quad \theta^{(t)}_{\text{merged}} = \theta^{(t-1)}_{\text{merged}} + \lambda \left(\theta^{(t)} - \theta^{(0)} \right), \tag{37}$$

where $\theta^{(t)}$ is the model parameters at step t, and $\theta^{(t)}_{\text{merged}}$ is the merged model parameters at step t.

Memory complexity of task arithmetic: As explained in Section 3.2, a continual model merging algorithm generally requires $O(|\theta|)$ memory, where $|\theta|$ represents the size of a single model. And task arithmetic can be implemented as a continual model merging method naturally. However, the most naive implementation of task arithmetic under the conventional model merging setting requires $O(T|\theta|)$ memory since it loads all the task-specific models and obtain the merged model as $\theta_{\text{merged}} = \theta^{(0)} + \lambda \sum_{i=1}^{T} \left(\theta^{(i)} - \theta^{(0)} \right)$.

Ties-Merging further extends the task arithmetic method by incorporating a systematic approach to handle parameter redundancy and sign conflicts during model merging [91]. This method ensures that the merged model retains the most relevant and consistent information from the individual task-specific models, thereby improving overall performance and robustness. By trimming redundant parameters, electing the most significant sign for each parameter, and performing a disjoint merge, Ties-Merging effectively reduces interference between tasks, leading to more stable and accurate results. Mathematically, Ties-Merging can be formalized as follows:

$$\left\{ \tau^{(i)}_{\text{Ties}} \right\}_{i=1}^{T} = \text{TiesMerging} \left(\left\{ \tau^{(i)} \right\}_{i=1}^{T} \right), \tag{38}$$

$$\theta_{\text{merged}} = \theta^{(0)} + \lambda \sum_{i=1}^{T} \tau^{(i)}_{\text{Ties}}, \tag{39}$$

where $\theta^{(0)}$ is the pre-trained model parameters, $\tau^{(i)} = \theta^{(i)} - \theta^{(0)}$ is the task vector for the i-th task, and $\tau^{(i)}_{\text{Ties}}$ is the trimmed and selected task vector for the i-th task. λ is a scaling factor that is similar to the one used in Task Arithmetic. We use the same scaling factor λ as in Task Arithmetic.

In our continual multi-task model merging experiments, we use the following update rule of the merged model at step t:

$$\theta^{(1)}_{\text{merged}} = \theta^{(0)} + \lambda(\theta^{(1)} - \theta^{(0)}), \quad \theta^{(t)}_{\text{merged}} = \theta^{(0)} + \lambda \left(\tau^{(t-1)}_{\text{Ties-merged}} + \tau^{(t)}_{\text{Ties}} \right), \tag{40}$$

where $\left\{ \tau^{(t-1)}_{\text{Ties-merged}}, \theta^{(t)}_{\text{Ties}} \right\} = \text{TiesMerging} \left(\left\{ \theta^{(t-1)}_{\text{merged}} - \theta^{(0)}, \theta^{(t)} - \theta^{(0)} \right\} \right)$.

D.3.2 Experimental Results

We conduct the continual multi-task model merging experiments on the three task groups using different sizes of CLIP-ViT models (ViT-B/32, ViT-B/16, and ViT-L/14). For each task group and

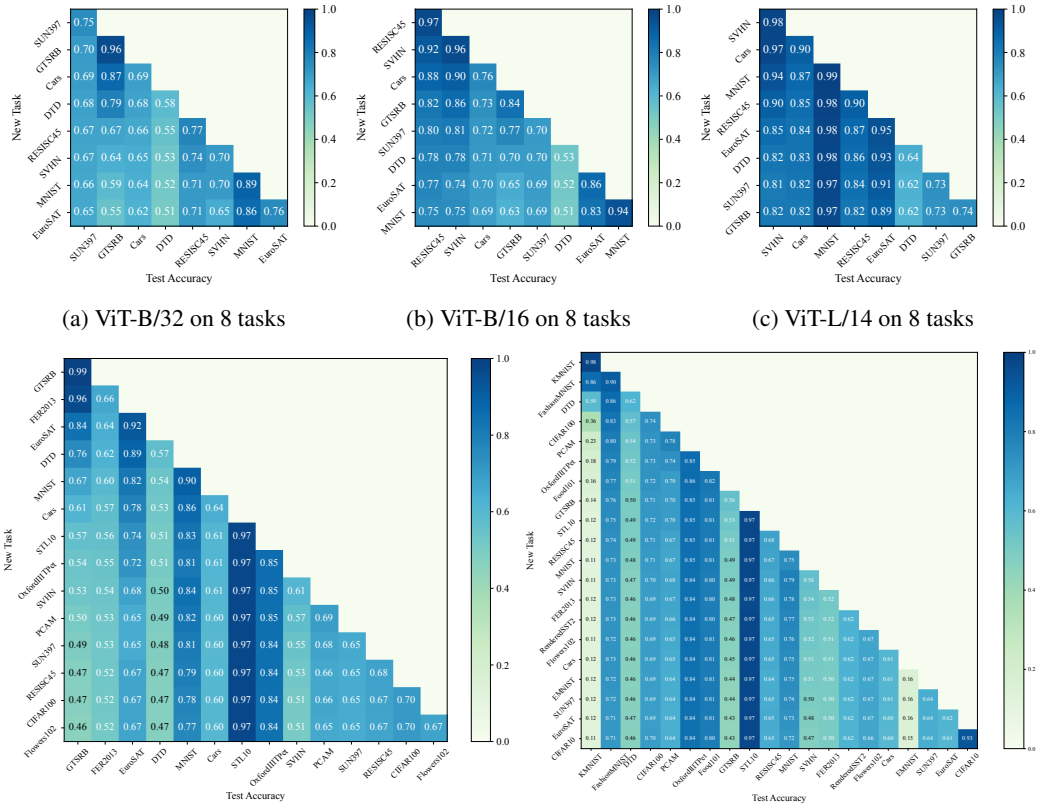

(a) ViT-B/32 on 8 tasks (b) ViT-B/16 on 8 tasks (c) ViT-L/14 on 8 tasks

(d) ViT-B/32 on 14 tasks (e) ViT-B/32 on 20 tasks

Figure 12: Here we show the accuracy matrix of the continual multi-task model merging using weight averaging for different model architectures and task sets. The order of the tasks is shuffled for each run.

model size, we repeat the experiment 10 times with different task orders to investigate the effect of task order on the performance of the continual multi-task model merging.

Accuracy matrix analysis. The accuracy matrix is structured as follows: each row corresponds to a new task-specific model incorporated into the merged model, while each column displays the test accuracy for individual tasks after merging. Specifically, for the i-th row, the j-th column represents the test accuracy of the j-th task for the merged model $\theta^{(i)}_{\text{merged}}$, i.e. $\text{ACC}_j(\theta^{(i)}_{\text{merged}})$. The diagonal elements represent the performance on the newly added task, while off-diagonal elements show how well the model maintains performance on previously learned tasks.

In Figure 12, we show the accuracy matrix of the continual multi-task model merging using weight averaging for different model architectures and task sets. These accuracy matrices reveals several key insights about the continual multi-task model merging process. First, we observe a general trend of accuracy degradation as more tasks are added. This suggests some degree of catastrophic forgetting occurs during continual merging. Second, larger models (ViT-L/14) show better resistance to this degradation compared to smaller models (ViT-B/32), maintaining higher accuracies across tasks. Third, when comparing task sets of varying sizes (8, 14, and 20 tasks), it becomes evident that maintaining consistent performance across all tasks grows increasingly challenging as the number of tasks expands. This is reflected in the generally lower accuracy values observed in the 14- and 20-task matrices. Finally, we note that the performance decline is particularly significant for certain tasks, such as KMNIST and EMNIST. This could be attributed to the fact that these tasks exhibit the greatest divergence from the pre-trained model and the other tasks in the set.

Per-task performance analysis. The experimental results in Table 4 and Table 5 demonstrate the effectiveness of different model merging approaches across three CLIP-ViT architectures (B/32,

Table 4: Test set accuracy of the pre-trained model and individual fine-tuned models on 14 different downstream tasks. For continual fine-tuning, we fix the random seed to 42, shuffle the task order, and report the average accuracy. For other methods, we repeat the experiment 10 times with different task orders. Here we abbreviate 'Continual' as 'C.' to save space.

Method	SUN397	Cars	RESISC45	EuroSAT	SVHN	GTSRB	MNIST
			CLIP-ViT-B/32				
C. Fine-Tuned	56.9	57.0	56.9	**79.2**	**89.7**	**81.0**	**93.4**
Average (SWA)	64.8±0.0	**60.4**±0.0	67.1±0.0	67.0±0.0	50.7±0.0	45.6±0.0	76.6±0.0
C. Task Arithmetic	64.4±0.0	59.6±0.0	67.3±0.0	67.8±0.0	54.0±0.0	50.0±0.0	80.7±0.0
C. Ties-Merging	64.8±0.8	59.7±1.7	68.9±4.7	62.5±3.1	50.1±2.8	53.3±7.2	80.8±5.0
OPCM (Ours)	**65.6**±0.4	57.9±1.0	**70.8**±1.8	77.8±2.1	69.9±1.8	62.3±1.0	92.2±1.0
			CLIP-ViT-B/16				
C. Fine-Tuned	64.3	**69.9**	66.2	**86.6**	**93.3**	**79.6**	94.9
Average (SWA)	67.5±0.0	65.9±0.0	71.5±0.0	71.1±0.0	64.6±0.0	54.1±0.0	82.6±0.0
C. Task Arithmetic	67.8±0.0	65.2±0.0	71.9±0.0	74.0±0.0	67.0±0.0	57.2±0.0	88.9±0.0
C. Ties-Merging	68.5±0.7	67.2±2.7	72.3±1.5	73.0±7.1	65.6±5.0	53.8±3.0	88.6±4.1
OPCM (Ours)	**68.8**±0.3	64.4±1.8	**78.7**±1.2	84.6±1.9	79.2±1.9	70.5±2.5	**95.4**±0.5
			CLIP-ViT-L/14				
C. Fine-Tuned	53.8	78.7	59.7	73.3	**89.0**	**99.0**	**98.8**
Average (SWA)	71.2±0.0	79.0±0.0	78.7±0.0	80.4±0.0	71.3±0.0	64.6±0.0	94.3±0.0
C. Task Arithmetic	71.6±0.0	78.4±0.0	79.3±0.0	80.3±0.0	72.4±0.0	67.9±0.0	95.3±0.0
C. Ties-Merging	72.2±1.2	78.4±0.8	81.5±4.9	79.4±5.3	72.4±4.0	66.1±2.8	94.6±1.5
OPCM (Ours)	**74.0**±0.2	**82.1**±0.4	**85.8**±0.8	**86.2**±1.3	84.4±1.8	85.1±1.3	97.7±0.2

Method	DTD	Flowers102	PCAM	Fer2013	OxfordIIITPet	STL10	CIFAR100
			CLIP-ViT-B/32				
C. Fine-Tuned	47.4	38.8	69.4	**70.4**	72.6	87.8	43.7
Average (SWA)	46.9±0.0	**67.4**±0.0	65.2±0.0	51.6±0.0	84.2±0.0	**97.2**±0.0	**70.4**±0.0
C. Task Arithmetic	48.0±0.0	66.1±0.0	69.8±0.0	53.1±0.0	84.2±0.0	96.6±0.0	69.2±0.0
C. Ties-Merging	48.2±1.6	66.0±2.2	67.6±2.8	54.3±3.1	84.0±0.7	97.1±0.3	69.9±2.3
OPCM (Ours)	**52.3**±0.7	65.6±0.6	**81.2**±1.2	60.5±0.5	**84.6**±0.2	96.7±0.2	68.5±0.5
			CLIP-ViT-B/16				
C. Fine-Tuned	46.4	42.0	64.1	**72.7**	84.1	90.8	56.5
Average (SWA)	47.2±0.0	72.5±0.0	63.2±0.0	54.1±0.0	90.4±0.0	**98.3**±0.0	73.4±0.0
C. Task Arithmetic	47.8±0.0	72.0±0.0	64.8±0.0	54.8±0.0	90.6±0.0	98.1±0.0	72.8±0.0
C. Ties-Merging	48.1±0.9	71.5±1.0	63.2±1.7	54.5±3.5	90.3±1.0	98.2±0.1	72.5±2.8
OPCM (Ours)	**51.8**±0.7	**74.5**±0.7	**83.9**±1.2	62.7±0.4	**92.7**±0.2	97.9±0.1	**73.8**±1.2
			CLIP-ViT-L/14				
C. Fine-Tuned	42.6	57.3	60.9	52.9	83.1	87.6	57.1
Average (SWA)	58.7±0.0	81.9±0.0	74.2±0.0	54.8±0.0	94.6±0.0	**99.3**±0.0	82.4±0.0
C. Task Arithmetic	59.8±0.0	81.9±0.0	71.1±0.0	56.1±0.0	94.8±0.0	99.0±0.0	82.3±0.0
C. Ties-Merging	59.3±1.1	81.6±1.5	72.8±1.9	57.3±1.8	94.6±0.4	99.2±0.2	82.9±1.2
OPCM (Ours)	**63.6**±1.1	**87.6**±0.3	**80.4**±0.9	**63.1**±0.4	**95.8**±0.1	99.2±0.0	**84.0**±0.5

B/16, and L/14) on 14 and 20 downstream tasks, respectively. It is observed that OPCM (the proposed method) outperforms other continual model merging approaches in a majority of tasks. For instance, on ViT-B/32, OPCM achieves the best performance on several tasks including SUN397 (64.4%), RESISC45 (66.0%), SVHN (66.1%), GTSRB (56.0%), MNIST (90.2%), and PCAM (80.2%), FER2013 (58.5%), CIFAR10 (92.8%), and RenderedSST2 (64.6%). The results also reveal that certain tasks, particularly EMNIST and KMNIST, remain challenging for all continual model merging methods, though OPCM generally maintains better performance even on these difficult cases. Furthermore, Continual Ties-Merging shows significant higher standard deviations compared to OPCM across multiple tasks and model arichitectures, indicating that Continual Ties-Merging is much more sensitive to the order of tasks are merged, leading to inconsistent performance across different task orderings.

In Table 6, we dive deeper into the comparison between continual fine-tuning and OPCM by examining the average accuracy over 10 different task orders for OPCM. Continual fine-tuning is extremely computationally intensive. For instance, in our 20-task experiments, each task requires

Table 5: Test set accuracy of the pre-trained model and individual fine-tuned models on 20 different downstream tasks. For continual fine-tuning, we fix the random seed to 42, shuffle the task order, and report the average accuracy. For other methods, we repeat the experiment 10 times with different task orders. Here we abbreviate 'Continual' as 'C.' to save space.

Method	SUN397	Cars	RESISC45	EuroSAT	SVHN	GTSRB	MNIST	DTD	Flowers102	PCAM
CLIP-ViT-B/32										
C. Fine-Tuned	53.9	38.2	64.7	**98.7**	45.4	34.4	86.7	**58.4**	57.5	67.7
Average (SWA)	64.2±0.0	**59.6**±0.0	64.8±0.0	60.9±0.0	47.3±0.0	43.1±0.0	71.8±0.00.0	46.4±0.0	**66.5**±0.0	63.9±0.0
C. Task Arithmetic	62.0±0.0	53.7±0.0	60.9±0.0	58.1±0.0	48.5±0.0	48.9±0.0	79.4±0.0	46.1±0.0	61.1±0.0	73.4±0.0
C. Ties-Merging	62.5±2.2	49.1±4.3	55.8±2.7	50.9±5.2	54.6±13.4	49.3±6.4	82.0±5.8	46.7±3.7	58.5±3.7	69.9±4.1
OPCM (Ours)	**64.4**±0.3	51.1±1.6	**66.0**±1.2	71.7±2.1	**66.1**±2.6	**56.0**±1.2	**90.2**±0.6	40.4±0.7	64.9±0.4	**80.2**±0.6
CLIP-ViT-B/16										
C. Fine-Tuned	62.7	58.0	67.6	**99.1**	46.0	29.2	93.9	**61.9**	64.1	75.2
Average (SWA)	67.1±0.0	**64.6**±0.0	69.3±0.0	63.4±0.0	62.4±0.0	52.0±0.0	80.7±0.0	46.6±0.0	71.8±0.0	63.1±0.0
C. Task Arithmetic	65.8±0.0	57.5±0.0	63.8±0.0	59.5±0.0	64.7±0.0	54.0±0.0	88.8±0.0	45.3±0.0	67.5±0.0	67.1±0.0
C. Ties-Merging	64.2±1.6	52.9±7.8	60.9±5.2	53.0±8.3	62.8±10.1	48.8±5.0	88.4±4.2	45.0±2.5	61.3±3.7	68.5±6.4
OPCM (Ours)	**67.9**±0.2	55.9±1.3	**73.7**±0.8	77.5±2.9	**74.4**±0.9	**63.2**±1.9	**94.1**±0.5	49.2±0.4	**72.3**±0.3	**79.6**±3.0
CLIP-ViT-L/14										
C. Fine-Tuned	69.5	73.6	78.3	**99.2**	59.3	49.3	**98.6**	**69.7**	83.2	**78.3**
Average (SWA)	70.7±0.0	77.7±0.0	76.4±0.0	75.3±0.0	69.5±0.0	62.1±0.0	93.7±0.0	57.7±0.0	80.0±0.0	73.6±0.0
C. Task Arithmetic	70.4±0.0	74.1±0.0	73.9±0.0	66.3±0.0	69.9±0.0	65.6±0.0	95.1±0.0	56.6±0.0	78.6±0.0	70.4±0.0
C. Ties-Merging	69.6±1.5	70.3±3.5	65.3±2.9	47.9±7.5	76.1±8.8	63.6±7.1	94.7±0.9	54.4±2.1	77.9±2.7	72.3±3.0
OPCM (Ours)	**73.1**±0.2	**78.3**±0.5	**82.4**±0.4	80.2±2.6	**80.8**±0.4	**80.4**±0.7	97.4±0.3	61.6±0.8	**84.8**±0.4	76.3±1.9

Method	FER2013	OxfordIIITPet	STL10	CIFAR100	CIFAR10	Food101	FashionMNIST	EMNIST	KMNIST	RenderedSST2
CLIP-ViT-B/32										
C. Fine-Tuned	58.3	68.5	86.7	40.2	70.5	50.0	**90.7**	**72.4**	**54.5**	54.5
Average (SWA)	50.2±0.0	**84.1**±0.0	**97.0**±0.0	**69.8**±0.0	92.7±0.0	**80.4**±0.0	71.3±0.0	15.0±0.0	11.5±0.0	61.8±0.0
C. Task Arithmetic	51.4±0.0	82.3±0.0	94.9±0.0	64.6±0.0	91.4±0.0	71.9±0.0	73.9±0.0	17.8±0.0	12.2±0.0	59.9±0.0
C. Ties-Merging	49.5±2.9	81.3±1.9	95.2±0.5	63.7±1.8	91.2±1.4	70.2±2.6	73.7±4.5	17.8±2.8	16.9±4.6	59.8±4.1
OPCM (Ours)	**58.5**±0.6	82.9±0.3	95.9±0.3	67.6±0.7	**92.8**±0.3	74.0±0.8	76.3±1.0	22.4±1.0	18.3±1.6	**64.6**±0.6
CLIP-ViT-B/16										
C. Fine-Tuned	**60.5**	84.5	90.5	38.8	73.6	61.9	**89.7**	**83.3**	**51.5**	**72.8**
Average (SWA)	50.9±0.0	89.6±0.0	**98.0**	72.9±0.0	94.2±0.0	**85.9**±0.0	73.3±0.0	15.6±0.0	12.4±0.0	62.5±0.0
C. Task Arithmetic	50.7±0.0	89.3±0.0	97.0±0.0	68.0±0.0	93.1±0.0	80.3±0.0	75.7±0.0	18.1±0.0	16.7±0.0	61.8±0.0
C. Ties-Merging	50.4±6.2	87.9±1.6	96.3±0.9	63.1±4.8	91.7±1.9	78.0±2.3	75.0±4.0	23.4±8.4	24.9±7.1	61.5±4.9
OPCM (Ours)	59.5±0.4	**91.8**±0.2	97.7±0.1	**73.2**±0.9	**94.7**±0.2	83.1±0.2	81.3±0.6	26.5±1.2	23.4±0.6	66.8±0.8
CLIP-ViT-L/14										
C. Fine-Tuned	**68.0**	92.1	94.5	60.5	85.7	74.8	**93.1**	**89.0**	**59.2**	**78.8**
Average (SWA)	52.7±0.0	94.2±0.0	**99.2**±0.0	81.7±0.0	97.0±0.0	90.7±0.0	77.4±0.0	16.1±0.0	10.4±0.0	66.1±0.0
C. Task Arithmetic	55.7±0.0	94.2±0.0	98.6±0.0	79.1±0.0	96.6±0.0	87.6±0.0	80.8±0.0	17.6±0.0	10.6±0.0	63.6±0.0
C. Ties-Merging	57.6±3.0	93.5±0.8	97.8±0.5	74.0±4.3	95.6±1.7	84.7±2.5	79.7±2.1	20.2±5.5	12.6±4.2	58.4±2.4
OPCM (Ours)	61.8±0.2	**95.4**±0.1	**99.2**±0.0	**83.0**±0.4	**97.8**±0.1	**90.9**±0.2	86.0±0.2	26.4±0.9	14.7±2.2	71.0±1.1

Table 6: Test set accuracy comparison between continual fine-tuning and OPCM across different sizes of CLIP-ViT models and task sets.

Experimental Setup	Continual Fine-tuning	OPCM (Ours, 10 runs)
ViT-B/32, 8 tasks	79.8	75.5±0.5, Min: 74.8, Max:76.5
ViT-B/16, 8 tasks	82.9	81.8±0.3, Min: 81.3, Max: 82.3
ViT-L/14, 8 tasks	90.0	87.0±0.4, Min: 86.6, Max: 87.7
ViT-B/32, 14 tasks	67.4	71.9±0.3, Min: **71.3**, Max: 72.5
ViT-B/16, 14 tasks	72.2	77.1±0.5, Min: **76.2**, Max: 77.8
ViT-L/14, 14 tasks	70.9	83.5±0.2, Min: **83.1**, Max: 83.8
ViT-B/32, 20 tasks	62.6	65.7±0.2, Min: **65.3**, Max: 66.0
ViT-B/16, 20 tasks	68.2	70.3±0.2, Min: **69.8**, Max: 70.7
ViT-L/14, 20 tasks	77.7	76.0±0.2, Min: 75.6, Max: 76.4

20-30 minutes of fine-tuning. A single complete run, therefore, takes 8-10 hours. Here we report continual fine-tuning results from single runs, the comparison with our method's statistical analysis reveals compelling insights: In 5 out of 9 experimental settings (highlighted in bold), even our method's minimum performance exceeds continual fine-tuning's single-run results. In the remaining cases, our method still achieves competitive results within 1-5% of continual fine-tuning. OPCM

achieves the performance with orders of magnitude lower computational cost, requiring only a few seconds versus 20-30 minutes per task for continual fine-tuning.

D.4 Ablation Studies

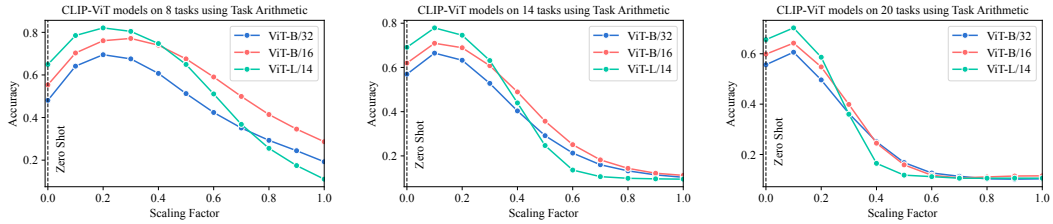

Figure 13: The average accuracy of Task Arithmetic with varying scaling factors.

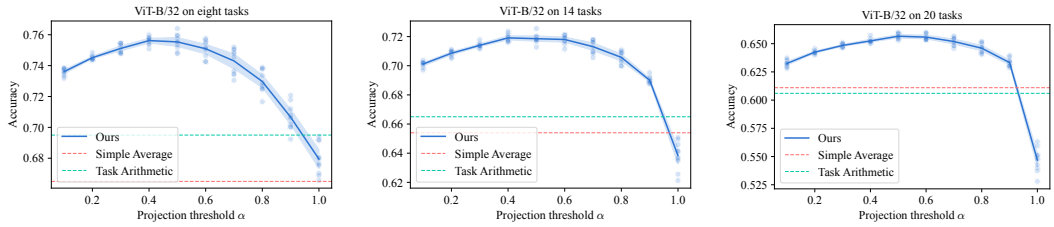

(a) ViT-B/32 on eight tasks (b) ViT-B/32 on 14 tasks (c) ViT-B/32 on 20 tasks

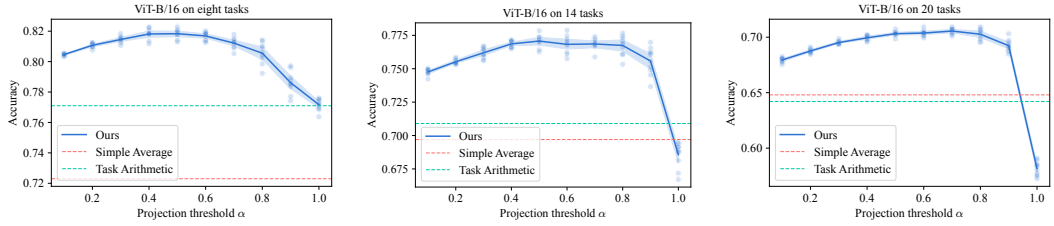

(d) ViT-B/16 on 8 tasks (e) ViT-B/16 on 14 tasks (f) ViT-B/16 on 20 tasks

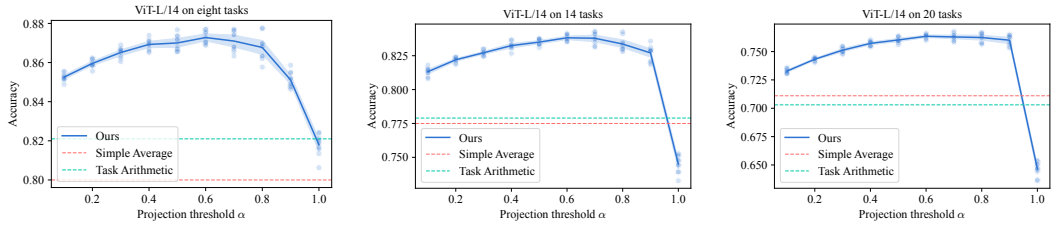

(g) ViT-L/14 on 8 tasks (h) ViT-L/14 on 14 tasks (i) ViT-L/14 on 20 tasks

Figure 14: The effect of the projection threshold α on the performance of the merged CLIP-ViT models.

In this section, we provide additional details on the ablation studies. We perform a grid search to systematically evaluate the scaling factor for Task Arithmetic and the projection threshold α for our proposed method. This analysis is conducted across a range of model architectures, including ViT-B/32, ViT-B/16, and ViT-L/14, as well as diverse task sets comprising 8, 14, and 20 tasks. The hyperparameter search space is as follows:

- Scaling factor for Task Arithmetic: {0.0 (zero-shot), 0.1, 0.2, 0.3, 0.4, 0.5, 0.6, 0.7, 0.8, 0.9, 1.0}.
- Projection threshold α for our proposed method: {0.1, 0.2, 0.3, 0.4, 0.5, 0.6, 0.7, 0.8, 0.9, 1.0}.

Figure 13 demonstrates the impact of adjusting the scaling factor in Task Arithmetic across various model architectures (ViT-B/32, ViT-B/16, and ViT-L/14) and task sets (8, 14, and 20 tasks). The findings reveal that model performance is highly dependent on the choice of scaling factor, with distinct optimal values identified for different task sets. Specifically, a scaling factor of 0.3 yields the best results for eight tasks, while a factor of 0.1 proves optimal for both 14 and 20 tasks. These results highlight the importance of carefully selecting the scaling factor to maximize performance in multi-task learning scenarios.

Figure 14 shows the influence of the projection threshold α on the merged model performance, revealing several key insights. First, the optimal value of α consistently lies within the range of 0.4 to 0.6, regardless of the number of tasks. Second, performance remains remarkably stable within this range, highlighting the robustness of our method to slight variations in the choice of α. Third, as the number of tasks increases from 8 to 20, the optimal range for α remains similar, demonstrating its scalability across different task complexities. Fourth, when compared to baseline methods such as Task Arithmetic, our approach consistently outperforms them across a broad spectrum of α values ($\alpha \leq 0.9$). These findings underscore the effectiveness of our method in facilitating efficient knowledge transfer and mitigating catastrophic forgetting, making it a reliable solution for continual multi-task model merging.

E Comparison With SOTA Conventional Model Merging Methods

Table 7: Comparison with conventional model merging methods on eight CLIP-ViT-B/32 models.

Method	SUN397	Cars	RESISC45	EuroSAT	SVHN	GTSRB	MNIST	DTD	Avg.
Conventional Model Merging									
Fisher Merging	66.7	64.0	72.2	91.6	69.0	64.3	83.5	53.7	70.6
RegMean	67.8	68.9	82.5	94.4	90.6	79.2	97.6	63.2	80.5
Task Arithmetic	57.1	55.7	64.9	76.7	77.9	68.5	96.1	47.2	68.0
Ties-Merging	67.1	64.2	74.1	76.8	77.7	69.4	94.1	54.0	72.2
Task-wise AdaMerging	58.6	56.9	69.8	82.4	70.3	58.9	97.2	55.3	68.7
Layer-wise AdaMerging	67.9	71.3	83.5	92.7	87.4	92.9	98.2	67.0	82.6
TSVM	67.6	71.6	84.7	93.4	91.9	92.5	98.9	63.8	83.1
Continual Model Merging									
C. Layer-wise AdaMerging	62.2	64.6	71.1	70.6	91.2	94.5	98.4	35.3	73.5
C. TSVM	59.9	59.5	64.0	64.7	87.9	86.1	99.5	34.3	68.5
Ours (10 runs)	66.2±0.5	63.5±0.5	78.0±2.2	86.5±1.9	82.4±1.3	74.3±1.4	96.9±0.7	56.4±1.3	75.5±0.5

In this study, we introduce the orthogonal projection-based continual merging (OPCM) method for scenarios where models *become available sequentially over time* rather than simultaneously. While conventional Model Merging such as AdaMerging assumes all expert models are available simultaneously. For a more comprehensive comparison, we also list the experiments results of some SOTA model merging methods on eight CLIP-ViT-B/32 models in Table 7. Our experimental results demonstrate that OPCM achieves superior performance compared to most conventional model merging approaches, despite operating under the more challenging continual setting where expert models are not simultaneously available, making it harder to resolve inter-task knowledge conflicts.

We also conducted experiments on AdaMerging [96] and TSVM [23] to compare its performance under the continual model merging setting. Specifically, we adapt the AdaMerging method and TSVM to the continual model merging setting by setting $\theta^{(0)}_{merged} = \theta^{(0)}$, $\theta^{(t+1)}_{merged} = \text{AdaMerging}(\theta_0; \theta^{(t)}_{merged}, \theta^{(t+1)})$ and $\theta^{(t+1)}_{merged} = \text{TSVM}(\theta_0; \theta^{(t)}_{merged}, \theta^{(t+1)})$, respectively. The results are shown in Table 7. The continual layer-wise AdaMerging and TSVM experiment was conducted with a single run using the following task sequence: SUN397, Cars, RESISC45, EuroSAT, SVHN, GTSRB, MNIST, and DTD. The results in the table demonstrate that AdaMerging in the continual merging setting achieves 73.5% average accuracy, which is notably lower than its performance in the conventional model merging setting (82.6%).